Helsinki University of Technology
Materials Physics Laboratory
Espoo 2003

STRUCTURE AND STABILITY OF VORTICES IN DILUTE BOSE-EINSTEIN CONDENSATES

Sami Virtanen

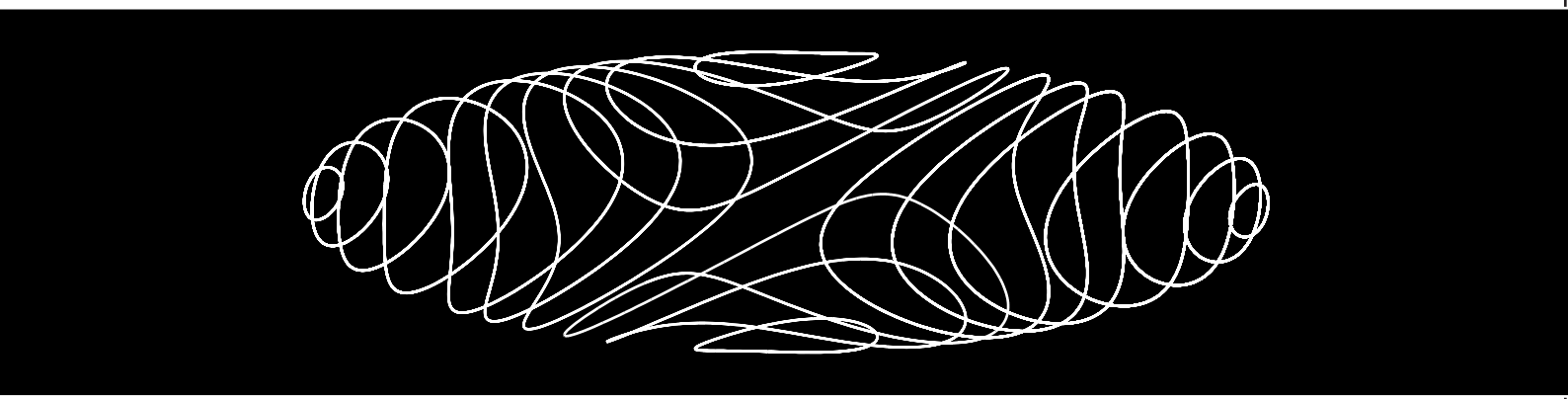

TEKNILLINEN KORKEAKOULU
TEKNISKA HÖGSKOLAN
HELSINKI UNIVERSITY OF TECHNOLOGY
TECHNISCHE UNIVERSITÄT HELSINKI
UNIVERSITE DE TECHNOLOGIE D'HELSINKI

Helsinki University of Technology Publications in Engineering Physics

Teknillisen korkeakoulun teknillisen fysiikan julkaisuja

Espoo 2003 TKK-F-A820

STRUCTURE AND STABILITY OF VORTICES IN DILUTE BOSE-EINSTEIN CONDENSATES

Sami Virtanen

Dissertation for the degree of Doctor of Technology to be presented with due permission for public examination and debate in Auditorium F1 at Helsinki University of Technology (Espoo, Finland) on the 4th of April, 2003, at 14 o'clock.

Helsinki University of Technology
Department of Engineering Physics and Mathematics
Materials Physics Laboratory

Teknillinen korkeakoulu
Teknillisen fysiikan ja matematiikan osasto
Materiaalifysiikan laboratorio

Distribution:
Helsinki University of Technology
Materials Physics Laboratory
P.O. Box 2200
FIN-02015 HUT
Tel. +358-9-451-5651
Fax. +358-9-451-3164
E-mail: Sami.Virtanen@hut.fi

ISBN 951-22-6426-9 (printed)
ISBN 951-22-6427-7 (pdf)
ISSN 1456-3320

Otamedia Oy
Espoo 2003

HELSINKI UNIVERSITY OF TECHNOLOGY
P.O. BOX 1000, FIN-02015 HUT
http://www.hut.fi

ABSTRACT OF DOCTORAL DISSERTATION

Author Sami Marko Mikael Virtanen

Name of the dissertation

Structure and Stability of Vortices in Dilute Bose-Einstein Condensates

Date of manuscript 12.11.2002 | Date of the dissertation 04.04.2003

☐ Monograph ☑ Article dissertation (summary + original articles)

Department Engineering Physics and Mathematics
Laboratory Materials Physics Laboratory
Field of research Vortices in Dilute Bose-Einstein Condensates
Opponent(s) Prof. Christopher J. Pethick
Supervisor Prof. Martti M. Salomaa
(Instructor)

Abstract

Since the first realizations of Bose-Einstein condensation in dilute alkali-atom vapours in 1995, these novel quantum gases have attracted wide interest. The main focus of the research has been on finding out the coherence and superfluidity properties of the condensates. From the theoretical point of view, these systems provide a rare possibility to model an interacting many-particle system exhaustively and quantitatively accurately from first-principles quantum field theories. However, the challenge of developing a correct and computationally feasible finite-temperature formalism still remains.

The coherence and superfluidity properties are intimately related to the existence and stability of quantized vortices. In this thesis, the structure and stability of vortex states in weakly interacting Bose-Einstein condensates is investigated within microscopic finite-temperature mean-field theories. An effective scheme for computationally solving the Bogoliubov-de Gennes quasiparticle eigenequations is developed, and applied to study the microscopic structure of vortex states in partially condensed vapours. In contrast to experimental observations and the predictions of the zero-temperature Bogoliubov approximation, stationary vortex states are found to be metastable within the self-consistent Popov approximation and its extensions even in the zero-temperature limit.

The reasons underlying this discrepancy are analysed in detail. A criterion for the validity of stationary mean-field approximations in modelling slowly time-dependent systems is derived, and applied to precessing off-axis vortex states. Under typical experimental conditions moving vortices are shown to be deformed due to the inability of the thermal cloud to follow the vortex core rigidly. Consequently, the validity of the commonly used stationary mean-field theories in describing such states is shown to be questionable. Finally, an analysis of uniformly precessing off-axis vortex states within a fully time-dependent Popov approximation is presented. Even dynamically deformed vortices are shown to become energetically metastable as the vortex core is partially filled with noncondensed gas in the course of thermalization. This self-stabilization mechanism of vortex states, shown to occur under very general circumstances, is an inherent property of all self-consistent formalisms having a structure similar to the Popov approximation. However, it is argued to be affected by the improper treatment of the noncondensate dynamics within these formalisms, and the need for a theory taking properly into account the coupled dynamics of the condensate and the noncondensate in modelling vortex states is emphasized. The computational scheme developed is also applied to investigate possibilities to energetically stabilize multiply quantized vortex states by piercing an externally rotated condensate with a blue-detuned laser beam.

Keywords Bose-Einstein condensates, vortices, finite-temperature effects

UDC 532.527:538.941 | Number of pages 70

ISBN (printed) 951-22-6426-9 | ISBN (pdf) 951-22-6427-7

ISBN (others) | ISSN 1456-3320

Publisher Helsinki University of Technology, Materials Physics Laboratory

Print distribution

☑ The dissertation can be read at http://lib.hut.fi/Diss/

Acknowledgements

This work has been carried out in the Materials Physics Laboratory at the Helsinki University of Technology during the years 1998–2002.

I wish to express gratitude to my supervisor Professor Martti Salomaa, the director of the laboratory, for suggesting the initial research topics, for supporting this work and for providing excellent facilities and conditions for the research. Special thanks belong to M.Sc. Tapio Simula for the patient conducting of the numerical computations, all the lively discussions, and the inexhaustible help in filling the laboratory with laughter. Furthermore, I wish to thank everybody in the Materials Physics Laboratory for contributing to such a pleasant working environment and atmosphere.

I am indebted to Professor Emeritus Eero Byckling and Professor Antti Niemi for encouragement, support and guidance during my first steps in theoretical physics. In addition, I cannot pass the opportunity to thank especially M.Sc. Tero Heikkilä, Dr. Jani Lukkarinen, Dr. Arttu Rajantie and Lic. Tech. Janne Salo for inspiring discussions on physics and mathematics during these years.

Financial support from the Foundation for Technology (Tekniikan edistämissäätiö) and the Academy of Finland via the Graduate School in Technical Physics are gratefully appreciated. The CSC–Scientific Computing Ltd is acknowledged for providing excellent computing facilities.

Finally, I want to warmly thank my parents Kaarina and Kalevi for their continuous support throughout my life.

Helsinki, October 2002

Sami Virtanen

List of Publications

This thesis is a review of author's work in the field of quantized vortices in Bose-Einstein condensates of dilute atomic gases. It consists of an overview and the following selection of author's publications in this field:

I. S. M. M. Virtanen, T. P. Simula, and M. M. Salomaa, *Structure and Stability of Vortices in Dilute Bose-Einstein Condensates at Ultralow Temperatures*, Phys. Rev. Lett. **86**, 2704–2707 (2001). © 2001 American Physical Society.

II. S. M. M. Virtanen, T. P. Simula, and M. M. Salomaa, *Comparison of mean-field theories for vortices in trapped Bose-Einstein condensates*, J. Phys.: Condens. Matter **13**, L819–L824 (2001). © 2001 IOP Publishing Ltd.

III. S. M. M. Virtanen, T. P. Simula, and M. M. Salomaa, *Adiabaticity Criterion for Moving Vortices in Dilute Bose-Einstein Condensates*, Phys. Rev. Lett. **87**, 230403-1–4 (2001). © 2001 American Physical Society.

IV. S. M. M. Virtanen and M. M. Salomaa, *Effect of the thermal gas component on the stability of vortices in trapped Bose-Einstein condensates*, J. Phys. B: At. Mol. Opt. Phys. **35**, 3967–3978 (2002). © 2002 IOP Publishing Ltd.

V. T. P. Simula, S. M. M. Virtanen, and M. M. Salomaa, *Stability of multiquantum vortices in dilute Bose-Einstein condensates*, Phys. Rev. A **65**, 033614-1–5 (2002). © 2002 American Physical Society.

VI. S. M. M. Virtanen and M. M. Salomaa, *Computing microscopic structures of inhomogeneities in superconductors*, Comp. Phys. Comm. **142**, 391–395 (2001). © 2001 Elsevier Science.

VII. S. M. M. Virtanen and M. M. Salomaa, *Multiquantum vortices in superconductors: Electronic and scanning tunneling microscopy spectra*, Phys. Rev. B **60**, 14581–14584 (1999). © 1999 American Physical Society.

VIII. S. M. M. Virtanen and M. M. Salomaa, *Midgap transition of domain walls in superconductors*, J. Phys.: Condens. Matter **12**, L147–L153 (2000). © 2000 IOP Publishing Ltd.

Throughout the overview, these papers are referred to by their Roman numerals.

Author's Contribution

The research presented in this dissertation has been carried out in the Materials Physics Laboratory at the Helsinki University of Technology during the years 1998–2002.

The author has had a central role in all aspects of this research work. He has developed all the analytical and numerical methods presented in Papers I–VIII. Papers I–IV are based on author's ideas and initiations, except for the initiation to apply the computational methods developed for superconductors to investigate vortex structures in dilute BECs. In addition, Papers VI–VIII are based on results obtained by the author.

The author has written all the Papers, except for Paper V and the introductory paragraph of Paper VII. He has, however, substantially contributed also in the writing process of Paper V. In addition, the author has presented the work at international conferences.

List of Abbreviations

The following abbreviations are used in the overview:

BA	Bogoliubov approximation
BCS	Bardeen-Cooper-Schrieffer
BdG	Bogoliubov-de Gennes
BEC	Bose-Einstein condensation/condensate
EEM	Eigenfunction expansion method
GP	Gross-Pitaevskii
HFB	Hartree-Fock-Bogoliubov
LCLS	Lowest core localized state
MQV	Multiply quantized vortex
PA	Popov approximation
PLA	Popov-like approximation
TF	Thomas-Fermi

Contents

1 Introduction

Regarding scientific interest and technological potential, superfluidity, superconductivity and lasing may be reckoned among the most important discoveries in the modern era of physics. Although observable on macroscopic length scales, these phenomena are fundamentally based on quantum mechanics. Especially, they are all manifestations of macroscopic occupation of a single quantum state.

The notion of macroscopic occupation of a quantum state dates back to 1924–1925, when Albert Einstein extended the statistical arguments presented by Satyendranath Bose [1] to systems with a conserved number of particles [2, 3]. Einstein soon recognized that an ideal gas of atoms obeying the resulting statistical distribution would condense into the ground state of the system at low enough temperatures. According to Einstein, a phase transition would occur at a critical temperature $T_{\rm BEC}$, below which a macroscopic number of atoms occupies the quantum state having the lowest energy. This phenomenon, subsequently termed Bose-Einstein condensation (BEC), is a unique, purely quantum-statistical phase transition in the sense that it occurs in principle even in noninteracting systems of bosonic particles.

In 1938, BEC was suggested by Fritz London to underlie the observed superfluidity of ^{4}He in its low-temperature liquid phase [4]. Although London's suggestion has recently been supported by neutron scattering experiments [5] and Monte Carlo simulations [6], the exact nature of BEC in superfluid ^{4}He has remained somewhat unclear due to strong interaction effects and consequent lack of a transparent microscopic theory. BEC is also closely related to the Bardeen-Cooper-Schrieffer (BCS) mechanism of superconductivity [7], which can be viewed as simultaneous formation and condensation of fermion pairs. In this generalized sense, the idea of bosonic condensation has been subsequently found useful in such diverse fields as condensed matter physics (superconductors, exciton condensates), nuclear physics (nucleonic condensation), astrophysics (meson condensates in neutron stars) and elementary particle physics (chiral vacuum condensate).

In the 1960's began an extensive search for BEC in a dilute, weakly interacting bosonic gas, in which the phenomenon would not be blurred by strong correlation effects of a liquid or a simultaneous BCS pairing of fermions. After decades of extensive efforts to observe BEC of excitons in semiconductors, or of spin-polarized hydrogen and laser-cooled alkali atoms (for a review, see Ref. [8]), the final breakthrough came in 1995. Anderson *et al.* at JILA*, soon followed by Davis *et al.* at MIT† and Bradley *et al.* at Rice University, managed to realize and observe convincing evidence for BEC in magnetically trapped ^{87}Rb [9], ^{23}Na [10] and ^{7}Li [11] atomic clouds, respectively, after combined laser and evaporative cooling to nanokelvin temperatures. These pioneering experiments launched an avalanche of research on the physics of dilute atomic condensates.

The gaseous condensates are in many ways complementary to previously known sys-

*Joint Institute for Laboratory Astrophysics, University of Colorado at Boulder.

†Massachusetts Institute of Technology.

tems exhibiting macroscopic quantum phenomena. Their interactions give rise to nonlinear phenomena not characteristic of laser fields, but are weak enough to allow high condensate fractions and to facilitate quantitative theoretical analysis based on perturbation theory, in contrary to the helium superfluids [12, 13]. On the other hand, in addition to being bosonic systems instead of fermionic, the quantities directly observable for gaseous condensates are quite different from the ones for superconductors. These differences render the dilute, trapped BECs a new class of many-particle systems, which has already yielded numerous experimental discoveries and offers an unprecedented testbench for developing thermal quantum field theories [14].

Regarding the experimental challenges to originally attain BEC in trapped atomic gases, these systems have turned out to be surprisingly robust and flexible. Diverse means to manipulate them—especially the strength and spatial dependence of the effective atomic interactions—render the ultracold gases ideal tools for studying complex physical phenomena in well-controllable systems. The phenomena already studied range from atom lasers [15] to quantum phase transitions [16], but these systems have been suggested to be utilized as laboratories to simulate and study for example cosmic strings [17], black holes [18] and self-gravitating gases [19].

Although dilute, the trapped atomic vapours are interacting, nonlinear systems. Their physics is consequently seldom exactly solvable, and also numerical approaches typically rely on approximate methods. Due to diluteness and the ultralow temperatures of the gases, mean-field approximation turns out to be a valid starting point for perturbation theory taking into account higher-order atomic correlations [12]. Because of inhomogeneity of trapped gases, even simplest mean-field approaches pose serious computational challenges at finite temperatures, and the majority of the theoretical analysis has been performed using the zero-temperature Bogoliubov approximation [20, 21]. The Bogoliubov approximation essentially neglects the effects of the thermal, noncondensed gas component and all higher-order correlations between the atoms. For dilute gases it yields in general excellent agreement with experiments in the zero-temperature limit. The corrections to the excitation spectra predicted by the lowest-order mean-field approximation are typically only of order a few per cent for temperatures $T \ll T_{\mathrm{BEC}}$ [22]. At higher temperatures, however, the thermal gas component becomes increasingly important and more refined approximations are needed.

The simplest finite-temperature extension of the Bogoliubov approximation, the so-called Popov approximation of the Hartree-Fock-Bogoliubov theory [23, 24], takes into account the thermal gas component in a self-consistent manner, but neglects all higher-order correlation effects and the coupled dynamics of the thermal and condensate components. The Popov approximation is in general quite accurate for temperatures $T \lesssim 0.6T_{\mathrm{BEC}}$, but closer to T_{BEC} discrepancies between its predictions and experimental data become obvious [25]. Much effort has been devoted to develop theories that consistently extend beyond the Popov approximation. Due to the modifications in the dynamical many-particle correlations caused by boson condensation, consistent mean-

field theories including the effects of higher-order correlations turn out to be difficult to formulate, and the challenge to develop a correct and computationally feasible theory still remains [24, 26].

Coherence and superfluidity properties are of fundamental interest in the physics of trapped, gaseous BECs. The interrelations between bosonic condensation, coherence and superfluidity are highly nontrivial in finite, interacting systems, and in addition to dilute BECs, important also for understanding the helium superfluids and high-temperature superconductors. The degree to which the weak atomic interactions do sustain superfluidity in gaseous BECs, and the coherence properties of these systems have been central issues under investigation. Usually the characteristic superfluidity properties, i.e. dissipationless, irrotational flow, reduced moment of inertia, vanishing viscosity, and various additional collective modes [27], are interpreted in terms of coherence and spontaneous phase-symmetry breaking: the system is essentially assumed to be describable with an order parameter having a well-defined phase. However, for finite systems at nonzero temperatures such a description is only approximate, and its validity an important issue to be investigated [28, 29].

Quantum phase coherence is typically manifested on microscopic length scales as the existence of quantized vortices, which are string-like topological defects in the complex-phase field. Quantized vortices are characteristic of macroscopic quantum systems: They have been extensively analysed in the context of the helium superfluids [30,31] and superconductors [32], and have an important role also in cosmology and astrophysics (cosmic strings [33], neutron stars [34]), nuclear and elementary particle physics (rotating nuclei [35]) and optics (optical vortices [36]). For dilute BECs, analysis of the existence and properties of quantized vortices and the development of methods to create them experimentally were rewarded in 2000 by the first realization and observation of vortices in condensed ^{87}Rb vapours [37]. The recent advances in creating vortices and observing their dynamics [38–43], together with foreseeable future experiments, are providing important information on the coherence and superfluidity properties of these systems. A crucial issue is the stability properties of vortex states—existence of stable, quantized vortices is a characteristic feature of superfluid behaviour.

Despite the extensive theoretical analysis of vortex states in dilute, trapped BECs [44], there still remain open questions. Due to computational challenges posed by the Popov formalism, the analysis has been undertaken almost exclusively within the Bogoliubov approximation. The effects of the noncondensate component on vortex structure, stability and dynamics have not been thoroughly studied. Such investigations could prove beneficial also in developing finite-temperature theories for these systems. For example, the large density gradients associated with vortex states provide stringent tests for theories based on approximations derived using the homogeneous gas limit [45–47].

The main objective of this thesis is to study the effects of the thermal component on the structure and stability of vortex states in dilute BECs, by using the finite-temperature Popov approximation and its extensions. In order to facilitate computation of the self-

consistent vortex structures in the low-temperature limit, numerical methods for efficiently solving the Bogoliubov-de Gennes quasiparticle eigenequations in effectively 1D configurations are developed. A combination of numerical and analytical methods is used to study the structure, stability and dynamical behaviour of vortex states within theories having the structure of the Popov formalism. In addition, possibilities to energetically stabilize multiquantum vortex states by using a laser field pinning potential are investigated.

Section 2 of this overview contains a description of the physical systems under consideration, and the theoretical frameworks generally used to model them. The main results on the structure and stability of quantized vortex states in trapped BECs (Papers I–V) are presented in Section 3, which also contains a description of general rotational properties of bosonic condensates and their relation to superfluidity, a brief review of the results obtained for pure condensates within the Bogoliubov approximation, and an account of the current experimental situation on vortex states. The numerical methods developed for solving the Bogoliubov-de Gennes quasiparticle equations for superconductors and Bose-Einstein condensates (Papers VI–VIII) are presented in Section 4. The overview is concluded with Section 5 summarizing the most important results obtained and their proper interpretation.

2 Dilute Atomic Vapours and Mean-Field Theory

Any first-principles theoretical description of an atomic gas or fluid faces two fundamental challenges: account of the atomic interactions and analysis of the ensuing many-body problem. In general, neither of these problems can be resolved exhaustively—on the contrary, one usually has to resort to poorly controllable approximations. Concerning the first issue, *ab initio* calculations yield binary interaction potentials between two atoms accurately only for the very lightest elements [48]. Higher than binary-order encounters complicate the situation even further, and a full, precise account of interactions is not available even for the lightest atoms. On the other hand, given the form of the interactions and the corresponding effective Hamiltonian of the system, the resulting many-body problem is seldom amenable to detailed quantitative analysis—usually the interactions and correlations between particles are too strong to allow the problem to be tackled by means of perturbation theory, for example. In the field of low-temperature physics, the helium superfluids are typical systems in this respect: for them the first-principles many-body problem is analytically intractable and the validity of approximate methods cannot be guaranteed. Various thermodynamical quantities, such as energy, pressure and condensate fraction can be computed by using simulative Monte Carlo methods [6], but such approaches do not yield detailed information on the excitation spectrum or dynamics of the system, and are feasible only for relatively small system sizes.

The dilute, ultracold atom vapours are exceptional in being interacting systems for which the *ab initio* quantum mechanical description can be formulated accurately and resolved using well-controllable approximations combined with experimental data. Firstly, it remarkably turns out that their interactions can be accurately modelled with a simple effective interatomic potential [49, 50]. Secondly, for dilute gases the resulting many-body problem can be tackled by analytic means. Many-particle effects alter the effective binary interactions from those in the vacuum, but for dilute vapours these modifications can be taken into account perturbatively [12]. In the conventional treatment, mean-field theory serves as a starting point to perturbation theory, in which higher-order particle correlations are taken into account. It is to be noted that this approach is not a simple weak-coupling perturbation expansion in the interaction constant that is assumed to be small—in fact, interactions in these systems are prominent in the sense that they substantially affect the density distribution of trapped gases, for example.

In Subsection 2.1, after a general account of trapped ultracold atomic gases under consideration, we briefly describe how the effective trapping potentials arise from the interactions of neutral atoms with electromagnetic fields, and how the interactions of ultracold atoms can be modelled in a simple, yet accurate way. In addition to describing the characteristic features of trapped atom vapours, these considerations are intended to motivate the effective low-energy Hamiltonian used as the starting point for first-principles theoretical models. The usual mean-field approaches and their extensions are described in Subsections 2.2 and 2.3, respectively.

2.1 System characterization

The dilute, ultracold gases in question typically consist of $N = 10^3$–10^{10} neutral alkali-metal (or hydrogen) atoms, which are controlled, manipulated and measured using magnetic and laser fields [51–53]. Alkali atoms are especially suitable for such purposes since their optical transitions can be excited with available lasers and their energy-level structure enables laser cooling to extremely low temperatures.

The alkali-atom vapours are isolated and confined by generating with magnetic and/or optical means typically an effectively harmonic trapping potential in a vacuum cell. Using various advanced cooling methods, typically laser cooling followed by evaporative cooling, the temperature of trapped gases can be lowered to the nanokelvin regime. At such temperatures the equilibrium phase of the alkalis is naturally a solid, and the gaseous systems have only a limited lifetime. This inherent metastability of ultracold gases poses a fundamental difficulty for reaching phase-space densities required for Bose-Einstein condensation. Fortunately, the molecular formation proceeds predominantly only via higher than binary-order collisions in order to effectively distribute the surplus energy released in the process. The ratio of such collisions to the binary collisions needed for thermalization depends on the density of the gas, and can be decreased by reducing it. This ratio is of crucial importance because it determines whether the gas has time to be evaporatively cooled and properly thermalized according to the appropriate quantum statistics before solidification. For typical maximum gas densities $n_{\max} \sim 10^{14}$ cm^{-3}, the lifetime of the gaseous phase is of order one minute, while the thermalization time scales are of order $\tau_{\text{ther}} \sim 10^{-2}$ s. Thus, thermalization can be arranged to be much faster than solidification.

The ground-state electron configuration of alkalis consists of closed shells and a single valence electron in an ns state. Since the electronic angular momentum vanishes, the total atomic angular momentum is the sum of the valence electron and nuclear spins, and in the absence of external electromagnetic fields the ground-state doublet is split only by the hyperfine interaction between the electronic and nuclear magnetic moments. The atomic excitations are "frozen" at sub-Kelvin temperatures and the atoms may be regarded in this respect as structureless composite particles, but the finite total spin implies them to have an internal degree of freedom.

The total spin also determines the quantum-statistical nature of these composite particles according to the spin-statistics theorem: particles with integer spin are bosons and obey Bose-Einstein statistics, and those with half-integer spin are fermions that obey Fermi-Dirac statistics [54]. Equivalently, since neutral atoms consist of $Z + A$ fermions and the atomic number Z is odd for alkalis, their quantum statistical nature is bosonic for isotopes with odd mass number A, and fermionic for even mass number isotopes. This quantum-statistical nature crucially affects the properties of atom vapours when they are cooled to low enough temperatures. Quantum statistical effects have been demonstrated by cooling separately trapped vapours consisting of bosonic and

fermionic isotopes of a given atomic species: At temperatures approaching the quantum degeneracy limit, the squeezing of the fermionic vapour ceases due to the Fermi pressure originating from the Pauli exclusion principle [55]. In contrast, bosonic vapours continue to compress with lowering temperature, until finally the maximum phase-space density attains values corresponding to Bose-Einstein condensation. For a uniform ideal gas in three dimensions, the critical phase-space density is given by $n\lambda_{\mathrm{dB}}^3 = 2.612$, where n is the density of the gas and $\lambda_{\mathrm{dB}} = (2\pi\hbar^2/Mk_{\mathrm{B}}T)^{1/2}$ the thermal de Broglie wavelength for atoms with mass M [54]. In finite systems, the thermodynamic BEC phase transition is somewhat smoothened, but for trapped mesoscopic vapours it is still an abrupt transition at a well-definable temperature. For typical experimental conditions with the alkalis, the transition temperature is of order $T_{\mathrm{BEC}} \sim 10$ nK – 1 μK. Below T_{BEC}, a macroscopic fraction of the gas occupies the collective ground state of the system and forms a phase-coherent condensate.

Trapping of neutral atoms

The usual atom traps and many advanced cooling techniques utilize the interaction of atoms with external magnetic or laser fields, or both [51–53]. Trapping of neutral atoms is typically based on shifting of atomic energy levels in an electromagnetic field—this shift corresponds to an effective external potential for an atom.

In an external magnetic field $\mathbf{B}(\mathbf{r})$, the level shift is due to the Zeeman interaction of the field with the magnetic moment of the atom. Due to the substantial difference in mass, the contribution of the nucleus to the atomic magnetic moment can usually be neglected. For ground-state alkali atoms, the magnetic moment is consequently determined by the spin of the valence electron. The eigenstates of the effective atomic Hamiltonian including the hyperfine and Zeeman interactions can be labeled with the quantum numbers F and m_{F} related to the total atomic spin in the zero-field limit and its projection in the direction of the magnetic field, respectively. The level splitting is given by the Breit-Rabi formula [56]. For typical field strengths used in the experiments, the hyperfine splitting substantially exceeds the Zeeman effect, and the magnetic field dependence may be linearized to yield for the atomic energy

$$E(F, m_{\mathrm{F}}) = E(F) + m_{\mathrm{F}} g_{\mathrm{F}} \mu_{\mathrm{B}} B, \tag{2.1}$$

where g_{F} is the Lande g-factor of the atom, μ_{B} Bohr's magneton, and B the magnetic field strength at the position of the atom. Depending on the sign of the factor $m_{\mathrm{F}} g_{\mathrm{F}}$, the states are termed high- or low-field seekers, for the obvious reason. It is to be noted that m_{F} is practically a good quantum number even for moving atoms, since at velocities corresponding to nanokelvin temperatures the atoms follow adiabatically changes in the direction of the magnetic field.

The atomic Zeeman effect can be utilized in trapping the atomic gas with an external magnetic field. In typical *magnetic traps*, the time-orbiting potential (TOP) and Ioffe-Pritchard traps being the most commonly used [53], the effective field magnitude in the

condensate volume can be accurately approximated by a harmonic potential having a field minimum at the trap center.* According to Eq. (2.1), such a field configuration provides for atoms in low-field seeking states a harmonic trapping potential

$$V_{\rm trap}(\mathbf{r}) = \frac{1}{2}M(\omega_x^2 x^2 + \omega_y^2 y^2 + \omega_z^2 z^2), \tag{2.2}$$

where M is the atomic mass and $\omega_i(m_F)$ are the classical harmonic oscillator frequencies. On the other hand, high-field seekers are expelled out of the trap. In order to have the same trapping potential for all atoms, in most experiments performed using magnetic traps the gas consists of atoms polarized in only one hyperfine state, i.e. the hyperfine degree of freedom is fixed.

Neutral atoms can also be manipulated with laser fields. Interaction of light with an atom gives rise to conservative and dissipative forces on the latter [59, 60]. In the alkali-gas experiments one usually utilizes the valence electron *ns*–*np* transition, which lies in the optical region. In the first-order dipole approximation, which is usually sufficient in the optical regime, the conservative force component arises from the interaction of the laser field with the dipole moment it induces to the atom. For laser frequencies slightly detuned from the transition, the resulting *dipole force* can be written as the negative gradient of the potential

$$V_{\rm dipole}(\mathbf{r}) = \frac{d^2}{\epsilon_0 c}\frac{\Delta I(\mathbf{r})}{\Delta^2 + (\hbar\Gamma_{np}/2)^2}. \tag{2.3}$$

Here $\Delta = \hbar\omega_{\rm laser} - (E_{np} - E_{ns})$ is the detuning of the laser, d the appropriate dipole matrix element between the states, Γ_{np} the linewidth of the excited state, and $I(\mathbf{r})$ the laser intensity. The shape of the potential is determined by the laser intensity profile. The potential is attractive for red detuning ($\Delta < 0$) and repulsive for blue detuning ($\Delta > 0$). Being a conservative interaction, the dipole force is naturally suitable for trapping purposes. The simplest such an *optical trap* is a focused red-detuned laser beam. In contrast to magnetic traps, optical traps do not require the atomic hyperfine degree of freedom to be fixed since the trapping potential is essentially independent of the magnetic substate. This allows investigation of multicomponent condensates composed of two or more coexisting hyperfine species.

The dissipative part of the atom – laser field interaction gives rise to the so-called *radiation pressure*. Radiation pressure is mainly utilized in laser cooling of atoms, but it is also used to compress the atom vapour in *magneto-optical traps*. In optical trapping it heats the gas by enhancing spontaneous emission processes, and in order to reduce heating, the detuning of the laser has to be kept rather large.

Atomic interactions at ultralow temperatures

Although the trapped atomic vapours are dilute, they are far from being ideal gases. Atomic interactions crucially affect the thermalization, equilibrium and dynamical prop-

*Due to Earnshaw's theorem, magnetic field cannot have a local maximum in free space [57, 58].

erties and lifetime of these systems, and a detailed account of the interactions is required in modelling them theoretically. In general, an accurate determination of atomic interactions constitutes an overwhelming problem. The dilute, ultracold gases are exceptional in that one can find a simple effective interaction potential that is expected to accurately model their atomic interactions.

As long as the binary interaction potential of structureless bosons is spherically symmetric and decays sufficiently rapidly at large interparticle separations, the binary collision properties in the low-energy limit are known to be described by a single parameter, the s-wave scattering length [61,62]. The same applies to elastic collisions of two bosonic, magnetically polarized alkali atoms.*† The energies up to which the s-wave contribution dominates the collision cross-section of alkalis correspond typically to microkelvin temperatures [48]—in the experimentally attainable nanokelvin regime neglect of other partial waves is thus well justified. The scattering lengths depend sensitively on the details of the atomic interaction potential, and can be calculated *ab initio* only for hydrogen with sufficient precision [63]. However, the s-wave scattering lengths of several atomic species can be determined experimentally with good accuracy, primarily via cold-atom photoassociation and rethermalization measurements [48]. In some cases, the energies of colliding atom resonant states can be tuned with an external magnetic field. Since the scattering length depends sensitively on such *Feshbach resonances*, it is possible to adjust the effective atomic interaction with external fields [64–66].

The total s-wave cross section of identical bosons can be approximated by the "effective range" low-energy form $\sigma(k) = 8\pi a^2/[(1-\frac{1}{2}k^2 a r_{\rm e})^2 + k^2 a^2]$, where $\hbar k$ is the relative momentum of colliding particles, a the s-wave scattering length, and $r_{\rm e}$ the "effective range" of the interparticle potential [62]. On the other hand, the pseudopotential [67]

$$V_{\rm int}(\mathbf{r},\mathbf{r}') = g\delta(\mathbf{r}-\mathbf{r}')\frac{\partial}{\partial r}r, \tag{2.4}$$

where the coupling constant g is related to the s-wave scattering length via

$$g = 4\pi\hbar^2 a/M \tag{2.5}$$

and $r = |\mathbf{r}-\mathbf{r}'|$ denotes the atomic separation, scatters only via the s-wave channel and yields $\sigma(k) = 8\pi a^2/[1+k^2a^2]$ for the total cross section. The pseudopotential $V_{\rm int}(\mathbf{r},\mathbf{r}')$ can thus be used as an effective low-energy binary interaction potential valid at least in the regime $kr_{\rm e}, ka \ll 1$. The scattering lengths of alkalis are typically a few nanometers, i.e. they are large in the atomic scale and often exceed $r_{\rm e}$ [49]—in such a case the validity criterion of the pseudopotential reduces to $ka \ll 1$. It is to be noted that when operating

*Purely s-wave collisions of *unpolarized* alkali atoms can be characterized by *two* scattering lengths, corresponding to the triplet and singlet pairing channels of their electronic spins.

†For identical fermions, the s-wave scattering length always vanishes due to the antisymmetry of the pair wave function. Spin-polarized fermionic atoms are thus "asymptotically non-interacting" in the low-energy limit, which complicates their cooling to ultralow temperatures.

on regular wave functions, the pseudopotential reduces to the simple contact interaction potential

$$V_{\rm int}(\mathbf{r},\mathbf{r}') = g\delta(\mathbf{r}-\mathbf{r}'). \tag{2.6}$$

Generally in many-particle systems higher than binary-order encounters can have an important contribution to interactions. However, their relative contribution is proportional to the *gas parameter* na^3 [67]. Essentially, the gas is regarded as dilute if $na^3 \ll 1$. For typical condensate densities $n = 10^{13}$–$10^{15}\mathrm{cm}^{-3}$, the gas parameter is less than 10^{-4} and higher-order collisions may be neglected. The elastic interactions of dilute ultracold bosonic atom vapours are thus expected to be accurately modelled by the simple effective potential (2.4) or (2.6). It is to be noted that the reduced form (2.6) presupposes that the high-energy degrees of freedom of the many-particle wave function have already been integrated out.

In addition to elastic collisions, composite particles with internal level structure can also interact inelastically. Inelastically colliding atoms usually escape from the trap due to spin flipping or simply because of the excess energy released in the process, and constitute a loss of atoms determining the trap lifetime. The most important inelastic processes in cold atom traps are collisions with vacuum impurity atoms, three-body recombination processes leading to molecule formation and spin-flip transitions arising from the coupling of atomic magnetic moments [50]. The rates of these processes depend on the experimental conditions and the atomic species used. However, alone the requirement that the thermalization rate given by elastic collisions has to substantially exceed the trap loss rate implies that inelastic processes can be accounted for only as a second-order effect which limits the trap lifetime, but otherwise does not affect the interaction properties of dilute vapours.

Effective Hamiltonian

The considerations presented above motivate choosing the effective low-energy Hamiltonian

$$\hat{H}_{\mathbf{\Omega}} = \int d\mathbf{r}\, \left[\hat{\psi}^\dagger(\mathbf{r},t)\mathcal{H}_{\mathbf{\Omega}}(\mathbf{r})\hat{\psi}(\mathbf{r},t) + \frac{1}{2}g\hat{\psi}^\dagger(\mathbf{r},t)\hat{\psi}^\dagger(\mathbf{r},t)\hat{\psi}(\mathbf{r},t)\hat{\psi}(\mathbf{r},t)\right] \tag{2.7}$$

as the starting point to model a dilute, trapped, bosonic atom vapour in a frame rotating with angular velocity $\mathbf{\Omega}$ with respect to the laboratory frame. Above, $\hat{\psi}(\mathbf{r},t)$ denotes the bosonic atom field operator, and the interactions are modelled with the contact potential given in Eq. (2.6). Furthermore,

$$\mathcal{H}_{\mathbf{\Omega}}(\mathbf{r}) = -\frac{\hbar^2\nabla^2}{2M} + V_{\rm trap}(\mathbf{r}) - \mathbf{\Omega}\cdot\mathbf{L} \tag{2.8}$$

is the single-particle Hamiltonian in the rotating frame ($\mathbf{L}$ is the angular momentum operator) for a particle confined by the trapping potential $V_{\rm trap}(\mathbf{r})$. The trapping potential is usually of the harmonic form of Eq. (2.2).

2.2 Bogoliubov and Popov mean-field approximations

The ultracold dilute atomic vapours provide a rare possibility to compare detailed experimental data to the predictions of first-principles finite-temperature quantum field theories describing an interacting many-particle system. The intimate interplay between theory and experiments has already advanced finite-temperature quantum field theories, and further progress in this direction is expected as improving experimental accuracy provides increasingly stringent tests for theoretical models.

Quantitative analysis of interacting, i.e. nonlinear, quantum field theories is a fundamental challenge in modern physics. Only few interacting field theory models in one and two spatial dimensions have been solved exactly. Typically, various mean-field approximations are used to circumvent the problem of solving the full many-body Schrödinger equation. For weakly interacting bosonic gases, even the simplest mean-field approaches yield in general good agreement with experiments [22]. Furthermore, the diluteness of these systems allows in principle developing systematic perturbative approaches to take into account higher-order interaction effects. The objective is to develop a quantitatively correct and computationally feasible formalism which can be used to calculate the physics to desired accuracy. Despite extensive efforts in this direction, such a theory is still lacking for dilute BECs [24, 26, 68].

Assuming the global $U(1)$ symmetry of the Hamiltonian (2.7) to be spontaneously broken in the BEC transition, the boson field operator is usually written in the mean-field approaches as the Bogoliubov decomposition

$$\hat{\psi}(\mathbf{r},t) = \Phi(\mathbf{r},t) + \tilde{\psi}(\mathbf{r},t), \tag{2.9}$$

where $\Phi(\mathbf{r},t) = \langle\hat{\psi}(\mathbf{r},t)\rangle$ is the macroscopic condensate wave function and $\tilde{\psi}(\mathbf{r},t)$ the noncondensate field operator for quantum and thermal fluctuations [20, 21].* It is to be noted that for nonvanishing condensate wave function the total particle number operator

$$\hat{N} = \int d\mathbf{r}\, \hat{\psi}^\dagger(\mathbf{r},t)\hat{\psi}(\mathbf{r},t) \tag{2.10}$$

no longer commutes with the Hamiltonian, which implies breaking of the particle-number conservation. This defect of the Bogoliubov decomposition can, however, be approximately compensated by using instead of $\hat{H}_{\mathbf{\Omega}}$ the grand-canonical Hamiltonian

$$\hat{K}_{\mathbf{\Omega}} = \hat{H}_{\mathbf{\Omega}} - \mu\hat{N}, \tag{2.11}$$

where the chemical potential $\mu = \mu(t)$ is chosen to yield the desired average number of particles. Essentially, this procedure turns out to be justified as long as the number of condensed particles $N_0 = \int d\mathbf{r}\, |\Phi(\mathbf{r},t)|^2$ is macroscopic, i.e. $N_0 \gg 1$.†

*The expectation values $\langle\cdots\rangle$ are intended to also average over time scales that exceed the duration of a typical atomic binary-collision process.

†It has recently been shown that essentially the same results can be derived by using more rigorous particle-number-conserving approaches [69–71]. Strictly speaking, the coherent symmetry-breaking state is not stationary but decays via quantum phase spreading, leading to collapses and revivals of the condensate wave function.

The dynamics of the system is determined by the Heisenberg equation of motion, which takes according to Eqs. (2.7), (2.10) and (2.11) the form

$$i\hbar\frac{\partial}{\partial t}\hat{\psi}(\mathbf{r},t) = \mathcal{K}_{\mathbf{\Omega}}(\mathbf{r},t)\hat{\psi}(\mathbf{r},t) + g\hat{\psi}^{\dagger}(\mathbf{r},t)\hat{\psi}(\mathbf{r},t)\hat{\psi}(\mathbf{r},t), \tag{2.12}$$

where $\mathcal{K}_{\mathbf{\Omega}}(\mathbf{r},t) = \mathcal{H}_{\mathbf{\Omega}}(\mathbf{r}) - \mu(t)$.* The expectation value of this equation yields the essentially exact equation of motion

$$\begin{aligned} i\hbar\frac{\partial}{\partial t}\Phi &= \mathcal{K}_{\mathbf{\Omega}}\Phi + g\langle\hat{\psi}^{\dagger}\hat{\psi}\hat{\psi}\rangle \\ &= \mathcal{K}_{\mathbf{\Omega}}\Phi + g\big[|\Phi|^2\Phi + \Phi^*\langle\tilde{\psi}\tilde{\psi}\rangle + 2\Phi\langle\tilde{\psi}^{\dagger}\tilde{\psi}\rangle + \langle\tilde{\psi}^{\dagger}\tilde{\psi}\tilde{\psi}\rangle\big], \end{aligned} \tag{2.13}$$

for the condensate wave function. Furthermore, subtraction of Eq. (2.13) from (2.12) yields correspondingly the equation of motion

$$\begin{aligned} i\hbar\frac{\partial}{\partial t}\tilde{\psi} &= \mathcal{K}_{\mathbf{\Omega}}\tilde{\psi} + g\big[\hat{\psi}^{\dagger}\hat{\psi}\hat{\psi} - \langle\hat{\psi}^{\dagger}\hat{\psi}\hat{\psi}\rangle\big] \\ &= \mathcal{K}_{\mathbf{\Omega}}\tilde{\psi} + g\big[2|\Phi|^2\tilde{\psi} + \Phi^2\tilde{\psi}^{\dagger} + \Phi^*\big(\tilde{\psi}\tilde{\psi} - \langle\tilde{\psi}\tilde{\psi}\rangle\big) \\ &\qquad + 2\Phi\big(\tilde{\psi}^{\dagger}\tilde{\psi} - \langle\tilde{\psi}^{\dagger}\tilde{\psi}\rangle\big) + \tilde{\psi}^{\dagger}\tilde{\psi}\tilde{\psi} - \langle\tilde{\psi}^{\dagger}\tilde{\psi}\tilde{\psi}\rangle\big] \end{aligned} \tag{2.14}$$

for the noncondensate operator.

Similar equations of motion can also be obtained for the noncondensate operator products appearing on the right-hand sides of Eqs. (2.13) and (2.14). Correspondingly, such equations contain still higher-order operator products, resulting ultimately in an infinite hierarchy of equations of motion [72]. In order to attain a feasible, closed formalism, the traditional way is to reduce the degree of fluctuation operator products by using mean-field approximations and approximate versions of Wick's theorem [73]. It is to be noted that this approach essentially relies on the diluteness assumption of the gas, since high-order correlations are expected to be weak in such systems.

The traditional "first-order" mean-field treatment is based on approximating the fluctuation operator products as

$$\begin{aligned} \tilde{\psi}^{\dagger}\tilde{\psi} &\simeq \langle\tilde{\psi}^{\dagger}\tilde{\psi}\rangle, \\ \tilde{\psi}\tilde{\psi} &\simeq \langle\tilde{\psi}\tilde{\psi}\rangle, \\ \tilde{\psi}^{\dagger}\tilde{\psi}\tilde{\psi} &\simeq 2\langle\tilde{\psi}^{\dagger}\tilde{\psi}\rangle\tilde{\psi} + \langle\tilde{\psi}\tilde{\psi}\rangle\tilde{\psi}^{\dagger}. \end{aligned} \tag{2.15}$$

Inserting into Eqs. (2.13) and (2.14), one finds the approximate equations of motion

$$i\hbar\frac{\partial}{\partial t}\Phi(\mathbf{r},t) = \mathcal{L}_{\mathbf{\Omega}}(\mathbf{r},t)\Phi(\mathbf{r},t) - gn_{\mathrm{c}}(\mathbf{r},t)\Phi(\mathbf{r},t) + g\tilde{m}(\mathbf{r},t)\Phi^*(\mathbf{r},t), \tag{2.16}$$

$$i\hbar\frac{\partial}{\partial t}\tilde{\psi}(\mathbf{r},t) = \mathcal{L}_{\mathbf{\Omega}}(\mathbf{r},t)\tilde{\psi}(\mathbf{r},t) + g\Phi^2(\mathbf{r},t)\tilde{\psi}^{\dagger}(\mathbf{r},t) + g\tilde{m}(\mathbf{r},t)\tilde{\psi}^{\dagger}(\mathbf{r},t), \tag{2.17}$$

*Note the slightly different notation in Papers I–IV.

where

$$\mathcal{L}_{\mathbf{\Omega}}(\mathbf{r},t) = \mathcal{K}_{\mathbf{\Omega}}(\mathbf{r},t) + 2gn(\mathbf{r},t) \tag{2.18}$$

and

$$\begin{aligned} n_{\mathrm{c}}(\mathbf{r},t) &= |\Phi(\mathbf{r},t)|^2, \\ \tilde{n}(\mathbf{r},t) &= \langle\tilde{\psi}^\dagger(\mathbf{r},t)\tilde{\psi}(\mathbf{r},t)\rangle, \\ n(\mathbf{r},t) &= n_{\mathrm{c}}(\mathbf{r},t) + \tilde{n}(\mathbf{r},t), \\ \tilde{m}(\mathbf{r},t) &= \langle\tilde{\psi}(\mathbf{r},t)\tilde{\psi}(\mathbf{r},t)\rangle \end{aligned} \tag{2.19}$$

denote the condensate, noncondensate and total densities, and the anomalous noncondensate average, respectively. Equation (2.16) is the time-dependent, generalized *Gross-Pitaevskii equation* for the condensate wave function [24,74–76]. On the other hand, Eq. (2.17) for the noncondensate operator is now bilinear and can be transformed into wave function equations by using the Bogoliubov transformation

$$\tilde{\psi}(\mathbf{r},t) = \sum_q \left[u_q(\mathbf{r},t)\alpha_q - v_q^*(\mathbf{r},t)\alpha_q^\dagger\right] \tag{2.20}$$

of the fluctuation operator in terms of the bosonic quasiparticle creation and annihilation operators $\alpha_q^\dagger$, α_q. Inserting the transformation into Eq. (2.17) implies the quasiparticle amplitudes $u_q(\mathbf{r},t)$ and $v_q(\mathbf{r},t)$ to satisfy the coupled equations of motion

$$i\hbar\frac{\partial}{\partial t}u_q(\mathbf{r},t) = \mathcal{L}_{\mathbf{\Omega}}(\mathbf{r},t)u_q(\mathbf{r},t) - g\left[\Phi^2(\mathbf{r},t) + \tilde{m}(\mathbf{r},t)\right]v_q(\mathbf{r},t), \tag{2.21a}$$

$$-i\hbar\frac{\partial}{\partial t}v_q(\mathbf{r},t) = \mathcal{L}_{-\mathbf{\Omega}}(\mathbf{r},t)v_q(\mathbf{r},t) - g\left[\Phi^{*2}(\mathbf{r},t) + \tilde{m}^*(\mathbf{r},t)\right]u_q(\mathbf{r},t). \tag{2.21b}$$

Furthermore, for the Bogoliubov transformation to be canonical, the amplitudes are to satisfy the normalization condition

$$\int d\mathbf{r}\,\left[u_q^*(\mathbf{r},t)u_{q'}(\mathbf{r},t) - v_q^*(\mathbf{r},t)v_{q'}(\mathbf{r},t)\right] = \delta_{qq'}, \tag{2.22}$$

which can be straightforwardly shown to be consistent with Eqs. (2.21). According to Eqs. (2.19) and (2.20), the noncondensate density and the anomalous average can be written in terms of the quasiparticle amplitudes as

$$\begin{aligned} \tilde{n}(\mathbf{r},t) = \sum_{qq'} \big[& f_{qq'}(t)\big(u_q^*(\mathbf{r},t)u_{q'}(\mathbf{r},t) + v_q^*(\mathbf{r},t)v_{q'}(\mathbf{r},t)\big) \\ & - 2\mathrm{Re}\{g_{qq'}(t)u_q(\mathbf{r},t)v_{q'}(\mathbf{r},t)\} + \delta_{qq'}|v_q(\mathbf{r},t)|^2\big], \end{aligned} \tag{2.23a}$$

$$\begin{aligned} \tilde{m}(\mathbf{r},t) = -\sum_{qq'} \big[& \big(2f_{qq'}(t) + \delta_{qq'}\big)v_q^*(\mathbf{r},t)u_{q'}(\mathbf{r},t) \\ & - g_{qq'}u_q(\mathbf{r},t)u_{q'}(\mathbf{r},t) - g_{qq'}^*v_q^*(\mathbf{r},t)v_{q'}^*(\mathbf{r},t)\big], \end{aligned} \tag{2.23b}$$

where

$$f_{qq'}(t) = \langle \alpha_q^\dagger \alpha_{q'} \rangle, \qquad g_{qq'}(t) = \langle \alpha_q \alpha_{q'} \rangle \tag{2.24}$$

are the normal and anomalous quasiparticle distribution functions, respectively. Finally, the chemical potential $\mu(t)$ is determined by the requirement that the integrated density equals the total particle number $N = \langle \hat{N} \rangle$:

$$N = \int d\mathbf{r}\, n(\mathbf{r}, t). \tag{2.25}$$

Equations (2.16), (2.21) and (2.23) together with equations of motion for the quasiparticle distribution functions determine the time evolution of the system in the Hartree-Fock-Bogoliubov (HFB) mean-field scheme [24, 77, 78]. The corresponding stationary equations, i.e. the time-independent generalized Gross-Pitaevskii equation

$$\mathcal{L}_{\mathbf{\Omega}}(\mathbf{r})\Phi(\mathbf{r}) - g n_{\mathrm{c}}(\mathbf{r})\Phi(\mathbf{r}) + g\tilde{m}(\mathbf{r})\Phi^*(\mathbf{r}) = 0, \tag{2.26}$$

and the quasiparticle eigenequations

$$\mathcal{L}_{\mathbf{\Omega}}(\mathbf{r})u_q(\mathbf{r}) - g\big[\Phi^2(\mathbf{r}) + \tilde{m}(\mathbf{r})\big]v_q(\mathbf{r}) = E_q u_q(\mathbf{r}), \tag{2.27a}$$

$$\mathcal{L}_{-\mathbf{\Omega}}(\mathbf{r})v_q(\mathbf{r}) - g\big[\Phi^{*2}(\mathbf{r}) + \tilde{m}^*(\mathbf{r})\big]u_q(\mathbf{r}) = -E_q v_q(\mathbf{r}) \tag{2.27b}$$

can be shown to diagonalize the Hamiltonian operator within a quadratic mean-field approximation, via the stationary Bogoliubov transformation corresponding to Eq. (2.20) [24]. Furthermore, the solutions of these equations minimize the free energy of the system (to a good approximation, see Ref. [79]) when the quasiparticle distribution functions obey the Bose-Einstein distribution, i.e.

$$\tilde{n}(\mathbf{r}) = \sum_q \big[n(E_q)\big(|u_q(\mathbf{r})|^2 + |v_q(\mathbf{r})|^2\big) + |v_q(\mathbf{r})|^2\big], \tag{2.28a}$$

$$\tilde{m}(\mathbf{r}) = -\sum_q \big[2n(E_q)u_q(\mathbf{r})v_q^*(\mathbf{r}) + u_q(\mathbf{r})v_q^*(\mathbf{r})\big], \tag{2.28b}$$

where

$$n(E_q) = \frac{1}{e^{E_q/kT} - 1}. \tag{2.29}$$

Equations (2.26) through (2.29) form a closed set determining the structure and excitation spectrum of the system in thermodynamic equilibrium at temperature T. For homogeneous BECs, the mean-field approach can be shown to be reliable only if the gas is sufficiently dilute, i.e.

$$na^3 \ll 1, \tag{2.30}$$

and the temperature is not too close to T_{BEC} [12]. Bosonic condensation modifies the effective atomic interactions in ways which can be found out in principle only by solving the many-body problem itself. However, for dilute gases these modifications are small in the sense that they do not invalidate the mean-field starting point, and can be taken into

account perturbatively. The criterion (2.30) is well satisfied under typical experimental conditions for trapped condensates, and in this respect the approximations underlying the HFB formalism are expected to be justified. On the other hand, the theory of phase transitions implies that fluctuations invalidating the mean-field approach grow in the vicinity of the BEC transition. For trapped systems, however, this needs not to be the case and mean-field approximations may be useful even through the transition region [68].

This HFB mean-field scheme has, however, certain shortcomings. First of all, it is plagued by ultraviolet and infrared divergences: The expression (2.28b) for the anomalous average turns out to diverge at high energies, and in the homogeneous limit $V_{\mathrm{trap}} = 0$ also infrared divergences arise in physical quantities. Ultraviolet divergences are typical for theories based on effective low-energy Hamiltonians, and the underlying reason for them in this case is the inappropriateness of the effective Hamiltonian (2.7) and especially the contact interaction potential (2.6) in the high-energy regime. On the other hand, the infrared divergences can be traced back to inaccuracies in approximating the noncondensate operator triple product according to Eqs. (2.15) [68].

Furthermore, the HFB approximation turns out to predict a spurious gap in the low-energy end of the excitation spectrum even in the homogeneous limit [24]. This energy gap violates the Hugenholtz-Pines theorem [80], and more generally Goldstone's theorem [81] which essentially states that spontaneously broken continuous symmetries give rise to bosonic modes that have a linear dispersion relation in the long-wavelength limit. The HFB scheme thus evidently fails to correctly predict the low-energy spectrum. The defective energy gap is also due to the failure of the triple-product approximation. In Eqs. (2.26) and (2.27) it is caused by the terms containing the anomalous average $\tilde{m} = \langle\tilde{\psi}\tilde{\psi}\rangle$ in much the same way as the energy gap in the BCS theory of superconductivity is caused by the pairing amplitude $\Delta \sim \langle\hat{\psi}_\uparrow\hat{\psi}_\downarrow\rangle$.

An obvious, although rather *ad hoc* way to modify the HFB formalism to get rid of the ultraviolet divergence and to conform it to Goldstone's theorem is to set explicitly

$$\tilde{m}(\mathbf{r}, t) \equiv 0 \qquad \text{(Popov approximation)} \tag{2.31}$$

in the HFB equations, instead of determining the anomalous average self-consistently according to Eqs. (2.23b) or (2.28b). This *Popov approximation* (PA) to the HFB theory, or HFB-Popov approximation, yields a gapless spectrum [23, 24]. The PA is equivalent to the finite-temperature Hartree-Fock theory in which all correlations between the particles, excluding the binary collisions corresponding to the interaction potential, are neglected. The PA has been recently given a firmer theoretical foundation [68], and is the most widely used finite-temperature formalism for dilute BECs.

For dilute gases in the low-temperature limit $T \ll T_{\mathrm{BEC}}$, the thermal gas fraction $\tilde{N}/N$, where $\tilde{N} = \int d\mathbf{r}\, \tilde{n}(\mathbf{r}, t)$, becomes negligible and the self-consistent HFB-Popov equations are often approximated by setting explicitly

$$\tilde{n}(\mathbf{r}, t) = \tilde{m}(\mathbf{r}, t) \equiv 0 \qquad \text{(Bogoliubov approximation)} \tag{2.32}$$

in the HFB formalism, instead of Eqs. (2.23) or (2.28). The resulting *Bogoliubov approximation* (BA) [20] consisting of the Gross-Pitaevskii equation and the Bogoliubov quasiparticle equations is computationally much less demanding than the PA. The BA, and especially the sole GP equation, is still the most commonly used model to analyse the physics of dilute BECs.

2.3 Beyond first-order mean-field theories

In addition to energetically averaged thermodynamic quantities, the experiments on dilute atomic BECs yield accurate information on the frequencies of individual collective modes of these systems. Such detailed spectral data provides unusually direct and stringent tests for the accuracy and correctness of the finite-temperature field theories.

At temperatures $T \ll T_{\text{BEC}}$, the Bogoliubov approximation yields in general excellent agreement with experimental results on the structure, excitation spectrum and dynamics of the condensate [22]. Furthermore, the finite-temperature Popov approximation agrees well with experimental data on collective modes for temperatures $T \lesssim 0.6T_{\text{BEC}}$, but for higher temperatures discrepancies between its predictions and experiments become evident [25, 82]. For spectrally averaged thermodynamic quantities, however, the PA works in general well up to temperatures $T \simeq T_{\text{BEC}}$.

The detailed reasons underlying the failure of the PA for temperatures approaching T_{BEC} are not known, but they are probably mainly due to the two main deficiencies of this approximation: Firstly, effects of the background gas on atomic correlations are not properly taken into account in the PA. Improper treatment of correlations is expected since they are represented in the HFB approximation by the anomalous average $\tilde{m}$, which is altogether neglected in order to obtain the PA. Secondly, formalisms based on the HFB approximation neglect the coupling of the condensate excitations with the thermal gas. Improper treatment of the coupled dynamics of the condensate and noncondensate is an inherent feature of first-order mean-field theories. In the previously given derivation this defect traces back to the coarseness of approximations (2.15). These approximations amount to neglecting the quasiparticle interactions, which are responsible for thermalization and the decay of excitations, for example.

A way to proceed beyond the PA and to lift the above-mentioned limitations is to evaluate the corrections to the exactly diagonalizable quadratic mean-field formalism using systematic second-order perturbation theory. The first *second-order theory* for a homogeneous Bose gas at zero temperature was developed by Beliaev in 1958 [83, 84]. An alternative pseudopotential method [85–87] was extended to second order in 1959–1960. Recently, these second-order theories have been generalized to describe trapped, inhomogeneous systems [68, 88].

In addition to including the lowest-order correlations in a way which yields a gapless spectrum (as required by Goldstone's theorem) and allows decay processes by partially taking into account the quasiparticle interactions, these systematic treatments also clar-

ify the validity criteria and accuracy of the first-order theories, and especially of the PA. They show that the mean-field theories serve as a valid starting point for a consistent and well-defined perturbation theory. However, due to computational challenges, the predictions of second-order theories have not yet been properly compared with experimental data.

As first approximations to take into account correlation effects neglected by the Popov approximation, the so-called G1 and G2 theories have been developed [46, 89]. Compared to the systematic second-order treatments, these formalisms are substantially less demanding computationally. In fact, they have structures similar to the Popov approximation, with the only difference in allowing the interaction couplings to depend on the correlation mean fields in a self-consistent manner. More specifically, the theories can be expressed in the form of the generalized Gross-Pitaevskii equation

$$\mathcal{L}'_{\mathbf{\Omega}}(\mathbf{r})\Phi(\mathbf{r}) - U_{\mathrm{c}}(\mathbf{r})n_{\mathrm{c}}(\mathbf{r})\Phi(\mathbf{r}) = 0, \tag{2.33}$$

and the quasiparticle eigenequations

$$\mathcal{L}'_{\mathbf{\Omega}}(\mathbf{r})u_q(\mathbf{r}) - U_{\mathrm{c}}(\mathbf{r})\Phi^2(\mathbf{r})v_q(\mathbf{r}) = E_q u_q(\mathbf{r}), \tag{2.34a}$$

$$\mathcal{L}'_{-\mathbf{\Omega}}(\mathbf{r})v_q(\mathbf{r}) - U_{\mathrm{c}}(\mathbf{r})\Phi^{*2}(\mathbf{r})u_q(\mathbf{r}) = -E_q v_q(\mathbf{r}), \tag{2.34b}$$

where

$$\mathcal{L}'_{\mathbf{\Omega}}(\mathbf{r}) = \mathcal{K}_{\mathbf{\Omega}} + 2U_{\mathrm{c}}(\mathbf{r})n_{\mathrm{c}}(\mathbf{r}) + 2U_{\mathrm{e}}(\mathbf{r})\tilde{n}(\mathbf{r}). \tag{2.35}$$

Comparison to Eqs. (2.18), (2.26) and (2.27) reveals that these equations reduce to the Popov approximation by setting $U_{\mathrm{c}}(\mathbf{r}) = U_{\mathrm{e}}(\mathbf{r}) \equiv g$. The G1 theory is obtained by choosing $U_{\mathrm{e}}(\mathbf{r}) \equiv g$ and $U_{\mathrm{c}}(\mathbf{r}) = g[1 + \tilde{m}(\mathbf{r})/\Phi^2(\mathbf{r})]$, and the G2 by choosing $U_{\mathrm{e}}(\mathbf{r}) = U_{\mathrm{c}}(\mathbf{r}) = g[1 + \tilde{m}(\mathbf{r})/\Phi^2(\mathbf{r})]$. The general structure of the equations implies that all these Popov-like approximations (PLAs) are gapless, but on the other hand none of them treats the noncondensate dynamically. In the G1 and G2, effects of the medium on atomic collisions are taken approximately into account through the effective, spatially dependent coupling functions $U_{\mathrm{c}}(\mathbf{r})$ and $U_{\mathrm{e}}(\mathbf{r})$. The two versions are based on different approximations for the momentum dependence of the full many-body T-matrix in the homogeneous gas limit [45–47].

3 Vortex States in Trapped BECs

Since the 1940's, the relationship between Bose-Einstein condensation and superfluidity has been extensively investigated mainly in order to understand the physics of superfluid ^{4}He. The term superfluidity generally refers to a complex of unusual hydrodynamic features, including the absence of viscosity, reduced moment of inertia, the occurrence of quantized vortices, infinite thermal conductivity, and additional sound modes in comparison to ordinary medium [27]. A characteristic property of superfluids is the *metastability of superflow*, i.e. the ability to support dissipationless, persistent currents practically indefinitely long [90]. Intuitively, these properties can be understood to stem from the macroscopic coherence related to Bose-Einstein condensation.

After the first experimental realizations of dilute, gaseous BECs in 1995, there has correspondingly been great interest to find out their coherence and superfluidity properties. These quantum gases differ substantially from the helium superfluids. Since metastability of superflow essentially depends on repulsive particle interactions, a fundamental question is whether the interactions in dilute BECs do sustain superfluidity and, more specifically, in which ways is superfluidity manifested in these mesoscopic, inhomogeneous systems.

The stability properties of vortex states is a crucial issue in this respect—the existence of stable, quantized vortices is a characteristic feature of superfluid behaviour, and can be seen as a manifestation of the metastability of superflow on microscopic length scales. Despite extensive theoretical analyses on this issue, there still exist open questions. A majority of the analysis has been conducted within the Bogoliubov approximation, and the effects of the noncondensate component on vortex stability and dynamics have remained somewhat unclear. The main objective of the research summarized in this thesis is to clarify these aspects on vortex stability in trapped, dilute, single-component BECs.*

In Subsection 3.1, we outline the main features of the response of coherent condensate matter to external rotation, and qualitatively describe the structure of quantized vortices in dilute BECs. In addition, we present the stability criteria relevant for vortex states, and briefly summarize the experiments on quantized vortices in gaseous condensates. The stability and dynamics of vortex states in pure condensates is discussed in Subsection 3.2. The effects of the thermal gas component on vortex states is the main topic of this thesis. It is the subject of Subsection 3.3, in which also the main results of Papers I–IV are presented. Finally, in Subsection 3.4 we analyse the conditions required to stabilize multiquantum vortex states on the basis of the results presented in Paper V.

*The hyperfine degree of freedom allows a rich variety of vortex structures in multicomponent condensates [91–93], and enables the existence of topological "textures" similar to those found in the A and B phases of ^{3}He [31]. In this thesis, however, we restrict to consider vortices only in single-component condensates.

3.1 Quantized vortices and metastability of superflow

The macroscopic coherence related to BECs implies these systems to have unusual rotational properties. A partially condensed gas or liquid can have contributions to its angular momentum from the center of mass motion, and from the intrinsic angular momenta of the incoherent noncondensate and coherent condensate components. Focusing on the latter, we note that a pure condensate can be described according to Eq. (2.9) by the macroscopic wave function

$$\Phi(\mathbf{r},t) = \sqrt{n_{\rm c}(\mathbf{r},t)}e^{iS(\mathbf{r},t)}, \tag{3.1}$$

where $n_{\rm c}(\mathbf{r},t) = |\Phi(\mathbf{r},t)|^2$ denotes the density of the condensate, and $S(\mathbf{r},t)$ is the complex phase of the wave function. Consequently, the condensate current density $\mathbf{j}_{\rm c} = (\hbar/2iM)(\Phi^*\nabla\Phi - \Phi\nabla\Phi^*)$ reduces to the form

$$\mathbf{j}_{\rm c} = n_{\rm c}\frac{\hbar}{M}\nabla S. \tag{3.2}$$

Identifying the factor multiplying the density of the condensate with its velocity field $\mathbf{v}_{\rm c}(\mathbf{r},t)$, the condensate flow is seen to be irrotational:

$$\nabla \times \mathbf{v}_{\rm c} = 0 \tag{3.3}$$

within the condensate volume.

Equation (3.3) strongly constrains the response of the condensate to rotation. In general, irrotationality results in a substantially reduced moment of inertia from its classical value [22,94]. One possibility for the condensate to respond to external rotation is to acquire angular momentum by exciting quantized vortices. Due to the single-valuedness of the condensate wave function, the line integral of the gradient of its phase along any closed path C in the condensate volume must be a multiple of 2π:

$$\Delta S = \oint_C \nabla S \cdot d\mathbf{l} = 2\pi m, \tag{3.4}$$

where m is an integer. If the condensate volume is singly connected, this integer has to vanish according to Stokes' theorem. On the other hand, it may be nonzero if C encompasses a curve along which $n_{\rm c}(\mathbf{r},t) = 0$. Such one-dimensional topological defects in the complex phase of the condensate wave function are called *quantized vortices*.

For simplicity, let us consider an axisymmetric, stationary vortex state with the condensate wave function of the form

$$\Phi(\mathbf{r}) = \Phi(r,z)e^{im\theta} \tag{3.5}$$

expressed in cylindrical coordinates $\mathbf{r} = (r,\theta,z)$. Here the integer $m \neq 0$ is the circulation quantum number, or *winding number*, of the vortex located along the z-axis. According

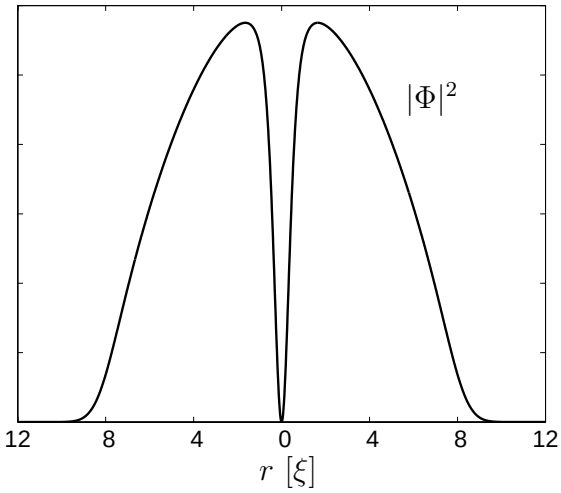

Figure 3.1: Density profile of an axisymmetric quantized vortex state in a radially trapped pure BEC. The ratio of the healing length ξ and the radius of the condensate is determined by the effective interaction parameter $\gamma = Na/a_{\rm ho}$, where $a_{\rm ho} = (\hbar/M\omega_\perp)^{1/2}$ is the harmonic oscillator length corresponding to trapping frequency $\omega_\perp$ in the radial direction.

to Eq. (3.2), the condensate circulates about the vortex axis with an azimuthal velocity component

$$v_\theta = \frac{1}{r}\frac{m\hbar}{M}, \tag{3.6}$$

which notably differs from 'classical' rigid-body rotation. The total angular momentum of the state is $L = Nm\hbar$, which corresponds to condensation of all the particles into a state having angular momentum $m\hbar$. The density profile can be found by solving the Gross-Pitaevskii equation (2.26) within the Bogoliubov approximation [95, 96]. Fig. 3.1 displays a typical density profile for a radially harmonically trapped condensate vortex state. Dimensional analysis of the GP equation shows that local inhomogeneities in the condensate wave function decay with a characteristic length scale given by the so-called *healing length*

$$\xi = \frac{1}{\sqrt{8\pi\bar{n}_{\rm c}a}}, \tag{3.7}$$

where $\bar{n}_{\rm c}$ is the average density surrounding the inhomogeneity. Especially, as the condensate density vanishes on the vortex axis, it heals back to the surrounding density essentially within a distance ξ from the center line (provided that the dimensions of the condensate exceed ξ). Instead of a single axisymmetric vortex, in the general case vortices may naturally be bent and the condensate may contain several vortices [97–100], but the previous analysis is still valid asymptotically in the vicinity of individual vortices.

Stability criteria

In discussing the stability of bosonic condensate states, we usually refer to their energetic stability. By definition, a physical system is *locally energetically stable*, or metastable, if its state is a local minimum of the free energy functional under the relevant external constraints. Furthermore, such a state is called *globally energetically stable*, or (thermodynamically) stable if the minimum is absolute. Another important stability concept is the *dynamical* or *Lyapunov stability*. Essentially, the system is dynamically stable if small perturbations to its state lead only to small deviations in its time development. Dynamic stability is a weaker condition than energetic one, since the theory of Hamiltonian dynamics implies that energetically stable systems are also dynamically stable [101].

A convenient way to determine the dynamical and local energetic stability of a stationary condensate state is to examine its excitation spectrum: If it contains an *anomalous* negative-energy *excitation* with respect to the condensate state, the system can lower its energy by transferring matter from the condensate state to the anomalous mode—in such a process also the free energy is decreased since the more uniform occupation number distribution implies increased entropy. Consequently, a condensate state containing an anomalous mode is energetically unstable, and decays with a time scale determined by dissipation rate. On the other hand, if the spectrum is strictly positive and the distribution functions obey the Bose-Einstein distribution, the free energy has a local minimum and the system is at least metastable. Finally, if the spectrum contains complex frequencies implying the corresponding states to be exponentially growing in time, the state is dynamically unstable and decays even in the absence of dissipation, and *vice versa*.

Energetics of rotating condensates

Whether a trapped condensate responds to rotation by nucleating vortices or by other means of acquiring angular momentum, can usually be determined by energetic considerations. In general, condensates with repulsive interactions turn out to favour creation of vortices and excitation of surface modes when rotated, while attractively interacting vapours favour centre of mass motion [97, 102–105]. In what follows, we focus on the stability of vortices and consequently restrict to consider the case of repulsive interactions. Especially, in order to investigate the metastability of superflow, the aim is to determine whether the system has (meta)stable states with nonvanishing angular momentum when it is *not* rotated externally.

Consider a system confined by a trap rotating with a constant angular velocity Ω. The trap is assumed to be at least slightly anisotropic, such that the condensate can exchange angular momentum with it. According to statistical mechanics, the system is equilibrated with respect to the frame in which the external potential is time-independent, i.e. in the frame rotating with the trap [54, 106]. The thermodynamically stable state

correspondingly minimizes the rotating frame free-energy functional

$$F_\Omega = F_{\rm lab} - \Omega L, \tag{3.8}$$

where $F_{\rm lab} = \langle \hat{H} \rangle - TS$ is the free energy in the nonrotating laboratory frame, and $L = \langle \hat{L} \rangle$ the angular momentum of the system in the direction of external rotation. We note in passing that a direct consequence of the minimization principle of F_Ω is that a state having angular momentum L and free-energy excess $\Delta F_{\rm lab}$ with respect to a stable state with vanishing angular momentum *may* become stable for rotation velocities exceeding the critical value

$$\Omega_{\rm c} = \frac{\Delta F_{\rm lab}}{L} \tag{3.9}$$

often called the *thermodynamic critical angular velocity*.

The stable states minimize the function $\mathcal{F}_\Omega(L)$, which we define to denote the absolute minimum of F_Ω for given total angular momentum L. They thus satisfy $\partial \mathcal{F}_\Omega / \partial L = 0$, or

$$\frac{\partial \mathcal{F}_{\rm lab}}{\partial L} = \Omega, \tag{3.10}$$

which implicitly determines the angular momentum $L(\Omega)$ of the stable state as a function of the trap rotation frequency—above, $\mathcal{F}_{\rm lab}$ denotes the absolute minimum of the free energy in the laboratory frame for given angular momentum (i.e. the free energy of the yrast states). Supposing first that $L(\Omega)$ is a smooth, invertible function, we may differentiate the relation (3.10) along the stable state trajectory to find

$$\frac{\partial^2 \mathcal{F}_{\rm lab}}{\partial L^2} = \frac{\partial \Omega}{\partial L} = I^{-1}, \tag{3.11}$$

where I denotes the moment of inertia $I = \partial L / \partial \Omega$ of the system. Since energetically stable states are also mechanically stable, their moment of inertia is positive, which implies also $\partial^2 \mathcal{F}_{\rm lab} / \partial L^2$ to be positive. On the other hand, in the absence of external rotation, the energetically most advantageous metastable states correspond to local minima of $\mathcal{F}_{\rm lab}$. Since the ground state in a static trap is naturally always irrotational, positivity of $\partial^2 \mathcal{F}_{\rm lab} / \partial L^2$ implies that there are no other local minima corresponding to finite angular momenta. Hence, we find that metastability of superflow implies $L(\Omega)$ to be discontinuous. By numerically minimizing the free energy within the Bogoliubov approximation, the angular momentum of a pure, weakly interacting, harmonically trapped condensate has indeed been found to have discontinuities with respect to Ω [97]. These correspond to transitions between states having different numbers of vortices, as expected.

However, although the discontinuity of $L(\Omega)$ is a necessary condition for metastability of superflow, i.e. stability of vortices in this case, it is not always sufficient. Intuitively, discontinuities in the angular momentum as a function of rotation velocity imply changes in the structure of the stable state, but this results in the existence of additional metastable states only if the structurally different configurations are separated by sufficient energy barriers. It is to be noted that even changes in the topological charge of

the state are not always associated with such energy barriers. A surprising counterexample is a harmonically trapped condensate in the weak-interaction limit: It turns out that quantized vortices in such a system are structurally unstable, and can disappear in the course of normal time-evolution even while the energy of the condensate is conserved [107]. In general, metastability of superflow can thus be sustained only if the system is sufficiently strongly interacting. For example, for a repulsively interacting condensate confined to an annular geometry, the states with different winding numbers are expected to be separated by energy barriers, giving rise to metastable rotational states. Indeed, this turns out to be the case [108–110]. The energy barriers are essentially due to the tendency of the repulsive interaction to favour uniform density distribution, i.e. nodes in the condensate density along which topological charge can unravel cost energy.

In simply connected geometries, however, the existence of such energy barriers is not guaranteed even in the presence of repulsive interactions. As described in Subsection 3.2, numerical analysis of the energy of pure condensates reveals that metastable vortex states exist only for finite trap-rotation velocities—especially, vortex states are unstable in staticly trapped pure condensates [97,98,111]. The role of the noncondensate component in this picture is, however, still somewhat unclear. Subsection 3.3 and Papers I–IV of this thesis focus on this aspect on the stability of vortices in dilute BECs.

Experimental realization of vortex states

Vortices have recently been realized and observed in experiments with dilute BECs. The first realization in JILA utilized an ingenious method, in which part of an irrotational condensate is directly transformed into a singly quantized condensate vortex state of another hyperfine species by selectively inducing transitions between the hyperfine states with a two-photon microwave field [37, 112]. When the microwave field coupling the hyperfine components is turned off, the system equilibrates to a state consisting of two phase-separated, but partially overlapping condensates. Finally, the irrotational component can be selectively removed, resulting in a single-component condensate in a vortex state. The vortex structure was observed by using nondestructive phase-contrast imaging technique. Subsequently, also the motion of the vortex core inside the condensate has been tracked. Essentially, in nearly spherical condensates vortices were observed to precess in circular orbits with constant radius about the condensate center [38].

A few months after the first realizations of condensate vortex states at JILA, a group at the Ecole Normale Supérieure (ENS) in Paris rotated a cigar-shaped single-component condensate with a laser beam in the longitudinal direction and observed the creation of vortex arrays of single-quantum vortices [39, 40]. At MIT regular vortex lattices hosting even of order one hundred vortices have been observed after applying laser-beam rotation to large condensates [41,42]. Recently, the ENS group has been able to obtain full-length images of vortices and to follow their dynamical evolution in prolate condensates [43].

Vortices and vortex rings have also been generated by creating turbulences in the

condensate with moving objects [42,113], via the decay of solitons [114,115], by exerting the condensate a torque with a rotating thermal cloud [116] and by rotating the condensate using a purely magnetic trap [117]. Recently, also multiquantum vortices with charges $m = 2$ and $m = 4$ have been created by using a topological phase engineering method [118–120].

Up to now, the conditions for nucleation of vortices [42, 116, 117, 121, 122] and their lifetime have been the central themes in the experimental study of vortex states in dilute BECs. The recent developments in engineering vortex states and obtaining full-length images of vortex lines pave the way for experiments yielding detailed information on the dynamical evolution and excitation modes of vortices.*

3.2 Stability and dynamics of vortices in pure condensates

Let us consider vortex states in condensates confined by an axisymmetric harmonic trap. With the z-axis oriented along the trap symmetry axis, the geometry of the trap and the condensate ground state are determined by the *asymmetry parameter*

$$\lambda = \frac{\omega_z}{\omega_\perp}, \tag{3.12}$$

where ω_z and $\omega_\perp = \omega_x = \omega_y$ are the axial and radial trapping frequencies, respectively.† The trap geometry is prolate for $0 < \lambda < 1$, spherical for $\lambda = 1$ and oblate for $\lambda > 1$. The case $\lambda = 0$ corresponds to an infinitely long cylindrical geometry.

The stability and dynamics of vortex states has been mainly addressed within the Bogoliubov approximation (cf. Subsection 2.2), which neglects the noncondensate component and assumes the system to be composed of a pure condensate. In the following, we first discuss the energetic stability of stationary, axisymmetric pure condensate vortex states, and then relate the results to the dynamical behaviour of off-axis vortices.

Axisymmetric vortex states

Let us first consider an axisymmetric vortex state with the vortex center line located along the symmetry axis of the trap and the condensate. Such a configuration is stationary, and its stability can consequently be determined from the excitation spectrum.

Using the BA, the spectrum is given by the HFB eigenequations (2.27) in the approximation (2.32). Due to the axial symmetry, the condensate wave function and the

*In addition to experimental investigation of quantized vortices, the superfluidity properties of gaseous BECs have also been studied and demonstrated by exciting the so-called "scissors mode" with a sudden rotation of an anisotropic trapping potential [123,124], by stirring the condensates with moving laser beams [125,126] and by moving them in corrugated lattice potentials [127].

†To be precise, the trap is assumed to be slightly anisotropic in the xy plane in order to be able to transfer angular momentum to the condensate. Basically, we neglect the effect of such a small anisotropy to the structure of the condensate state.

quasiparticle amplitudes may be chosen to have the form $\Phi(\mathbf{r}) = \Phi(r,z)e^{im\theta}$ and

$$\begin{aligned} u_q(\mathbf{r}) &= u_q(r,z)e^{i(q_\theta+m)\theta}, \\ v_q(\mathbf{r}) &= v_q(r,z)e^{i(q_\theta-m)\theta}, \end{aligned} \tag{3.13}$$

where m is the number of circulation quanta enclosed by the vortex, and the integer q_θ denotes the angular momentum quantum number of quasiparticles. Inserting this Ansatz into the Eqs. (2.26) and (2.27) yields effectively 2D eigenequations from which the condensate wavefunction, quasiparticle amplitudes and energies can be computed. In the case $\lambda = 0$, the Ansatz may be further reduced to $\Phi(\mathbf{r}) = \Phi(r)e^{im\theta}$ for the condensate state and

$$\begin{aligned} u_q(\mathbf{r}) &= u_q(r)e^{iq_z z}e^{i(q_\theta+m)\theta}, \\ v_q(\mathbf{r}) &= v_q(r)e^{iq_z z}e^{i(q_\theta-m)\theta}, \end{aligned} \tag{3.14}$$

for the quasiparticles, where q_z denotes the axial wave number of quasiparticles. The cylindrical case is consequently computationally only one-dimensional.

The quasiparticle spectrum of axisymmetric singly-quantized ($m = 1$) vortex states in repulsively interacting pure condensates is always real [128], and such states are consequently always dynamically stable.* On the other hand, multiquantum vortex states with $m \geq 2$ generally exhibit eigenmodes with complex frequencies corresponding to the dissociation instability of the vortex into m single-quantum vortices [128, 131]. Due to the dynamic instability of multiquantum vortices, we consider here only singly quantized vortices. We return to this issue in Subsection 3.4, where we discuss the stabilization of multiquantum vortices using additional laser field pinning potentials.

Already the first computations of the spectrum for singly quantized vortex states confined by an irrotating trap with $\lambda = \sqrt{8}$ (corresponding to time-orbiting potential traps) revealed that the lowest quasiparticle mode with $q_\theta = -1$ is anomalous, i.e. it has a negative energy but positive norm [132]. The corresponding mode was observed to be anomalous also in the cylindrical geometry with $\lambda = 0$ [133]. The negative-energy mode is seen in Fig. 3.2, which presents the lowest part of the quasiparticle spectrum within the BA. The existence of the negative-energy mode was soon shown to be a general feature of staticly trapped vortex states, and an interpretation of this anomalous mode was presented [111]. Essentially, excitation of this mode was argued to result in displacement of the vortex from the condensate center and the mode itself to correspond precession of the vortex line about the trap symmetry axis. In the presence of dissipation mechanisms and an initial perturbation to break the axisymmetry, the system could lower its energy by continuously transferring matter from the condensate state to this anomalous mode, resulting in spiralling of the vortex to the outskirts of the condensate and, eventually,

*In traps suitably asymmetric about the vortex axis even singly-quantized vortices can have imaginary frequency modes, implying them to be dynamically unstable against tilting of the vortex line with respect to the trap axis [129, 130].

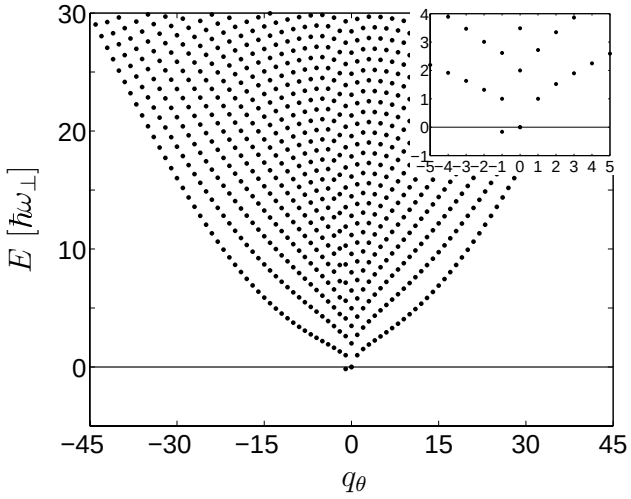

Figure 3.2: The low-energy part of the quasiparticle energy spectrum within the BA for a cylindrically trapped ($\Omega = 0$) condensate penetrated by a single-quantum vortex line. Only states with axial wave number $q_z = 0$ are shown. The physical parameter values are the same as in Papers I–II.

its annihilation. Thus, the existence of the anomalous mode would imply unstability of vortex states.

In the cylindrical case $\lambda = 0$ the lowest excitations with $q_\theta = -1$ for various values of q_z are so-called *Kelvin modes*, which are helical deformations of the vortex line with wave number q_z [30,134]. As expected, the density distributions $\rho_q(\mathbf{r}) = |u_q(\mathbf{r})|^2 + |v_q(\mathbf{r})|^2$ (cf. Eq. (2.28)) of these modes are strongly peaked in the vortex core. The longest wavelength Kelvin modes are anomalous, the most negative energetic being the mode with $q_z = 0$. Fig. 3.3 displays the density distributions of this so-called *lowest core localized state* (LCLS) and the condensate vortex state. The LCLS corresponds to rigid precession of the vortex about the trap axis. The angular velocity and the direction of precession are determined correspondingly by the modulus and the sign of the mode frequency $\omega_{\rm LS} = E_{\rm LS}/\hbar$, where $E_{\rm LS}$ denotes the energy of the lowest state, i.e. the LCLS. Especially, the negative sign of $E_{\rm LS}$ implies the vortex to precess in the direction of the condensate vortex flow [129,135,136]. In the ideal gas limit, the negativity of $E_{\rm LS}$ is obvious, since the Bogoliubov equations imply the lowest Kelvin mode to be the irrotational ground state of the system, which the axisymmetric vortex state exceeds in energy by $\hbar\omega_\perp$. For repulsively interacting condensates the situation is more complicated, but by using the Thomas-Fermi approximation it can be analytically shown that the anomalous mode energy approaches zero from below for increasing interaction parameter $\gamma = Na/a_{\rm ho}$ [137] (see also Ref. [138]).

In physically relevant finite geometries with $\lambda > 0$, the axial quantum number is discrete and the number of anomalous modes always finite. In analogy with the cylindrical

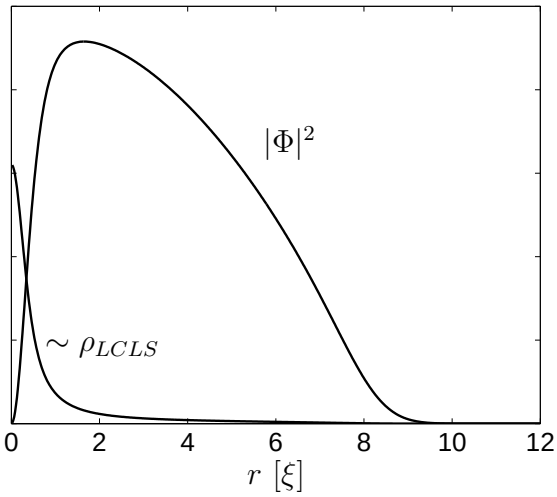

Figure 3.3: Density distributions of the LCLS and the condensate vortex state. The LCLS is strongly localized into the vortex core region. The relative scale for the densities is arbitrary.

geometry, the even z-parity anomalous modes* have angular momentum $-\hbar$ with respect to the condensate vortex state [129, 139, 140]. The number of such modes depends on the form of the trap: Oblate, spherical and slightly prolate geometries yield only one anomalous mode corresponding to precession of a slightly curved vortex line about the trap axis. However, for increasing prolateness parameter λ the energy $E_{\rm LS}$ of the lowest mode, the LCLS, becomes more negative and additional anomalous modes appear with more complicated z dependence. These additional anomalous modes correspond to precession of a deformed vortex. For long, cigar-shaped condensates the LCLS corresponds to bending of the vortex near its endpoints, where the local condensate density is low. Correspondingly, its energy is substantially lower than expected from the peak density at the center of the condensate. For cigar-shaped condensates, the existence of the anomalous modes corresponding to small radial displacement and strong bending of the vortex line suggests that for rapid enough external rotation the ground state of the system should be a bent vortex instead of an axisymmetric state. Indeed, this has been verified by numerically minimizing the GP energy functional for rotating traps [100, 141–143].

Although axisymmetric pure condensate vortex states are seen to be energetically unstable in static traps, it is to be noted that they can be stabilized by rotating the trap [144]. For externally rotated axisymmetric condensates the Bogoliubov equations imply the quasiparticle energies to transform due to Doppler effect as

$$E_q(\Omega) = E_q(0) - \hbar q_\theta \Omega, \tag{3.15}$$

where $E_q(\Omega)$ is the excitation energy in the frame rotating with the angular velocity Ω.

*We do not consider odd z-parity modes, because they are not associated with displacement of the vortex from the condensate center, but rather correspond to tilting of the vortex line with respect to the trap symmetry axis.

Since the system is thermalized with respect to the frame co-rotating with the trap, the vortex state becomes metastable for rotation frequencies exceeding the value

$$\Omega_{\rm m} = |\omega_{\rm LS}|, \tag{3.16}$$

at which the LCLS is lifted to positive energies in the rotating frame.* Due to lowering of the LCLS energy, the required metastability frequency $\Omega_{\rm m}$ increases for increasing trap prolateness.

Off-axis vortices

The linear eigenmode analysis of axisymmetric vortex states in principle describes the stability and dynamics of the vortex only infinitesimally close to the trap symmetry axis. Consequently, it is important to find out whether the results of the linear analysis hold for off-axis vortices at finite distances from the trap axis. However, because of the nonstationary nature of such states and the nonlinear dynamical behaviour of the condensate wave function, their analysis is both analytically and computationally more challenging [146].

For simplicity, let us again first consider the cylindrical case $\lambda = 0$. The existence of the negative-energy mode associated with infinitesimal displacement of the vortex from the condensate center suggests that also finite displacements of the vortex reduce the energy of the system. The change in the free energy per unit length induced by the vortex as a function of its displacement d from the trap axis can be calculated analytically in the Thomas-Fermi (TF) limit $\gamma = Na/a_{\rm ho} \gg 1$ by neglecting the effect of the vortex to the condensate density profile [136]. The result

$$\Delta E(\zeta, \Omega) = \frac{8\pi}{3}\mu\xi^2 n_0 (1-\zeta^2)^{3/2}\left[\ln\left(\frac{R_\perp}{\xi}\right) - \frac{4}{5}\frac{\mu\Omega}{\hbar\omega_\perp^2}(1-\zeta^2)\right], \tag{3.17}$$

where $R_\perp$ is the TF condensate radius in the radial direction, n_0 the maximum density of the corresponding irrotational condensate, and $\zeta = d/R_\perp$ the fractional displacement of the vortex, is presented in Fig. 3.4 for different trap rotation frequencies. The result is qualitatively correct also for condensates for which the TF limit is not justified, as has been verified by explicit numerical analysis of the GP equation [98, 147, 148].† As expected on the basis of the linear analysis, for nonrotating traps the vortex free energy has a local maximum at the trap axis. Furthermore, it decreases monotonically as a function of the vortex displacement, indeed implying the tendency of the vortex to

*Simultaneously, other quasiparticle energies are assumed to remain positive in the rotating frame. This turns out to be the case for singly quantized vortices in a finite range $\Omega_{\rm m} < \Omega < \Omega_{\rm nucl}$, where $\Omega_{\rm nucl}$ is the critical vortex nucleation frequency determined by the Landau criterion for surface excitations [145] (see also Paper V).

†Strictly speaking, even these analyses are approximate in the sense that they do not properly take into account the asymmetric distortion of the condensate velocity field related to the displacement of the vortex from the trap symmetry axis.

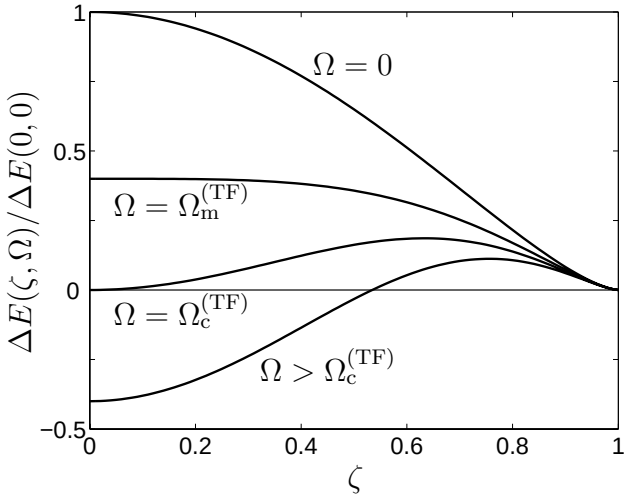

Figure 3.4: Energy of the vortex state as a function of the vortex displacement within the TF approximation for various values of the trap rotation velocity.

escape the condensate. On the other hand, the free energy curves also suggest that vortices can be stabilized by rotating the trap, as also expected from the analysis of the quasiparticle energies. At the metastability frequency $\Omega_{\rm m} \simeq \Omega_{\rm m}^{\rm (TF)}$ the axisymmetric vortex state becomes locally stable. Consequently, for $\Omega \gtrsim \Omega_{\rm m}^{\rm (TF)}$ slightly off-axis vortices are attracted to the trap center, which is then a local energy minimum. For rotation velocities $\Omega \gtrsim \Omega_{\rm c}^{\rm (TF)}$, the vortex state is globally stable.*

The gradient of the energy as a function of vortex position gives rise to an effective conservative force acting on the vortex in the radial direction. Part of this force is related to condensate density gradients: Since the density is locally suppressed in the core region, the vortex effectively feels a buoyancy force directed towards lower condensate densities [151]. Also, the asymmetric distortion of the condensate velocity field due to vortex displacement from the trap axis contributes to this conservative net force [146].

Despite the radial force acting on the vortex, in a pure condensate its motion in the radial direction is prohibited by the conservation of energy. Formally, this results from the Hamiltonian nature of the bare GP equation, which does not have dissipative terms. In the dynamical evolution a pure condensate state is thus restricted to move along constant energy manifolds, implying off-axis vortices in the cylindrical geometry to precess in circular orbits with constant radius. Note that such a motion is in agreement with the eigenmode analysis of axisymmetric vortex states. For off-axis vortices, it may be interpreted in terms of the *Magnus effect* [30, 152–154]: A cylinder moving with

*It is to be noted that these results hold qualitatively also for vortex states of superfluid ^{4}He in a cylindrical container [149, 150]. However, the curvature of free energy as a function of vortex displacement decreases for increasing cylinder radius, implying vortices in macroscopic cylinders to be practically stable even when the cylinder is not rotated.

velocity $\mathbf{v}$ in a homogeneous, incompressible, inviscid fluid having a potential flow with circulation $\boldsymbol{\kappa}$ about the cylinder experiences an effective *Magnus force*

$$\mathbf{F}_{\mathrm{Mag}} = -\rho(\mathbf{v} - \mathbf{v}_{\mathrm{L}}) \times \boldsymbol{\kappa}, \tag{3.18}$$

where ρ is the density of the liquid and $\mathbf{v}_{\mathrm{L}}$ its ambient velocity far from the cylinder. If the relative velocity $\mathbf{v} - \mathbf{v}_{\mathrm{L}}$ is constant in time, the Magnus force balances the resultant external force acting on the cylinder, giving rise to drifting of the cylinder in the direction orthogonal to the applied external force. Similarly, an off-axis vortex acted by a resultant force in the radial direction drifts along a circular trajectory about the condensate center. Using Eq. (3.18) as an estimate for the vortex precession angular velocity ω_{pr}, and neglecting the condensate ambient velocity (essentially, this amounts to neglecting the asymmetric distortion in the condensate velocity field), one finds

$$\omega_{\mathrm{pr}} = \frac{F_r}{2\pi\hbar M R_{\mathrm{pr}} n_c}; \tag{3.19}$$

here F_r is the net radial force acting on the vortex, R_{pr} the radius of the precession trajectory, and n_c the condensate density in the vicinity of the vortex. This estimate agrees rather well with the results obtained by numerically integrating the time-dependent GP equation [147]. Qualitatively, the precession frequency is an increasing function of the precession radius R_{pr}, primarily due to the lower condensate density outside the condensate center. On the other hand, for small precession radii the precession frequency approaches ω_{LS}, in agreement with the linear eigenmode analysis.

Analysis of off-axis vortex dynamics in finite geometries with $\lambda > 0$ is computationally challenging, and not much work has been done so far in this direction. Especially for strongly prolate geometries the mixing of several anomalous precession modes results in complicated behaviour, from which simpler modes are difficult to resolve [140, 147]. However, the qualitative features of vortex dynamics in numerical simulations agree with the results obtained within linear eigenmode analysis.

In conclusion, while harmonically trapped pure condensate vortex states are energetically unstable, the nondissipative condensate dynamics results in stability of vortices due to the absence of dynamical instabilities for singly quantized vortices. Consequently, off-axis vortices move in closed trajectories and never escape the condensate. However, this picture has to be modified for real systems which always have noncondensed gas present, giving rise to dissipative effects.

3.3 Effects of the noncondensate component on vortex states

The pure-condensate assumption is always only an approximation for real condensates. At finite temperatures, part of the system is noncondensed, with the noncondensate fraction approaching unity near T_{BEC}. In fact, because of quantum fluctuations, the noncondensate fraction is finite for interacting systems even at zero temperature. Consequently, concerning especially the properties of quantized vortices, it is interesting and

important to find out how the results obtained for pure condensates are modified when the noncondensate is taken into account. Despite the active theoretical investigation on the properties of vortex states in dilute BECs, notably few analyses on the noncondensate effects have been reported. The aim of the research presented in this thesis was primarily to clarify this aspect on the physics of vortex states in trapped BECs.

Essentially, the noncondensate modifies the pure condensate picture in two ways. Firstly, the coupling to the thermal cloud affects the physics of the condensate by providing it a dissipation mechanism. In addition, the interactions between the condensate and the noncondensate components modify the excitation spectrum and the structure of inhomogeneous states from those for a pure condensate.

In this Subsection, we analyse the relevance and importance of these effects for vortex states. After a brief account on the influence of dissipation on vortex dynamics, we concentrate in presenting the main results of Papers I–IV, and relating them to the existing literature. First, results on the structure and stability of vortex states within the self-consistent Popov approximation and its gapless extensions G1 and G2 are presented. The surprising but obvious discrepancy between the predictions of these HFB-type formalisms and the experimental observations of vortex states is the main subject of the following analysis. All the computational results presented in this Subsection correspond to the physical parameter values given in Ref. [155], unless explicitly stated otherwise.

Dissipative vortex dynamics

The thermal cloud has an important effect on the dynamics of the condensate by providing it a dissipation mechanism. The interaction between the condensate and the noncondensate components enables exchange of energy and momentum between them, resulting in damping of the condensate collective modes as opposed to the behaviour of the pure condensate. Especially, the noncondensate component affects vortex dynamics by imposing a friction force $\mathbf{F}_{\rm n}$ for moving vortices. This friction force is proportional to the relative velocity of the vortex line with respect to the noncondensate, and arises from collisions between the vortex and the normal-component quasiparticles. In the homogeneous limit it may be written in the form [153, 156]

$$\mathbf{F}_{\rm n} = -D(\mathbf{v} - \mathbf{v}_{\rm n}) - \tilde{n}(\mathbf{v} - \mathbf{v}_{\rm n}) \times \boldsymbol{\kappa}, \tag{3.20}$$

where $\mathbf{v} - \mathbf{v}_{\rm n}$ is the velocity of the vortex line with respect to the thermal gas and $D > 0$ is the longitudinal friction coefficient, the magnitude of which depends on the details of the vortex-quasiparticle interactions. Comparing to Eq. (3.18), the second term can be identified with the Magnus force component due to the thermal gas.

In a static, nonrotating trap the normal component velocity $\mathbf{v}_{\rm n}$ may be assumed negligible, and consequently only the longitudinal term opposing vortex motion is dissipative. For moving vortices, this longitudinal drag force combined with the Magnus effect gives rise to a velocity component in the direction of the net conservative force acting on the

vortex. Consequently, a moving vortex gradually drifts towards local energy minima. In a nonrotating trap, this leads to spiralling of the vortex outwards from the condensate center [156, 157]. Simultaneously, its velocity grows due to the proportionality of the balancing Magnus force to the density of the gas. Finally, as the velocity of the vortex exceeds the local sound velocity in the condensate, the vortex is annihilated by phonon (quasiparticle) emission. In contrast to the pure-condensate approximation analysed in the previous section, the energetically unstable vortices thus in fact decay because of the dissipative interaction with the thermal cloud always present in the system. However, because of the diluteness of gaseous BECs, dissipation may be so weak that the lifetime of vortices due to dissipation exceeds the condensate lifetime itself [156]. Also in this respect the dilute BECs fundamentally differ from superfluid ^{4}He.

Structure and stability of vortices within the Popov approximation

In addition to providing a dissipation mechanism for the condensate, the noncondensate also modifies the pure-condensate excitation spectrum and the structure of inhomogeneous states. In principle, these modifications could also affect the stability of vortex states.

The effect of the thermal gas on the structure and stability of vortices was first investigated by Isoshima and Machida, who computed self-consistent solutions for axisymmetric, irrotationally trapped, cylindrical ($\lambda = 0$) vortex states at finite temperatures within the Popov approximation (cf. Subsection 2.2) [155]. For sufficiently high temperatures, they indeed found the excitation spectrum to be positive and thus the vortex state to be stabilized. However, due to computational difficulties associated with iteration towards self-consistent solutions, the authors were unable to investigate the stability in the low-temperature region $T \lesssim 0.3T_{\mathrm{BEC}}$. In Paper I, an effective computational scheme based on high-order finite-difference discretization combined with an implicit Arnoldi method (cf. Section 4) was applied to survey this low-temperature region. Quite surprisingly, the vortex state was found to be energetically stable within the PA even in the zero-temperature limit. Fig. 3.5 displays the energy of the LCLS mode for low temperatures: It vanishes in the zero-temperature limit, but is well-behaved and positive for all temperatures below T_{BEC}, signalling the vortex state to be locally energetically stable. This result sharply contrasts the picture of vortex unstability given by the Bogoliubov approximation.

The structure of the vortex state is presented in Fig. 3.6, which displays the condensate and thermal component density profiles at various temperatures. The effect of the repulsive interactions is seen in the density profiles: the thermal gas is concentrated in regions with small condensate density. Especially in the low-temperature limit, the noncondensate is strongly localized to the vortex core region void of the condensate.

The energetic stabilization of the vortex state is directly related to this partial filling of the vortex core region with the thermal gas. Essentially, the thermal gas acts in the

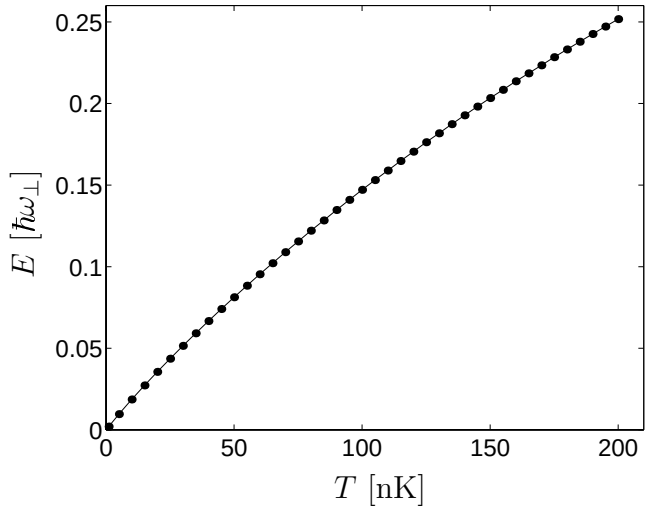

Figure 3.5: Energy of the lowest excitation, the LCLS, in the low-temperature limit within the PA. The finite positive value the lowest excitation energy implies the vortex to be locally energetically stable.

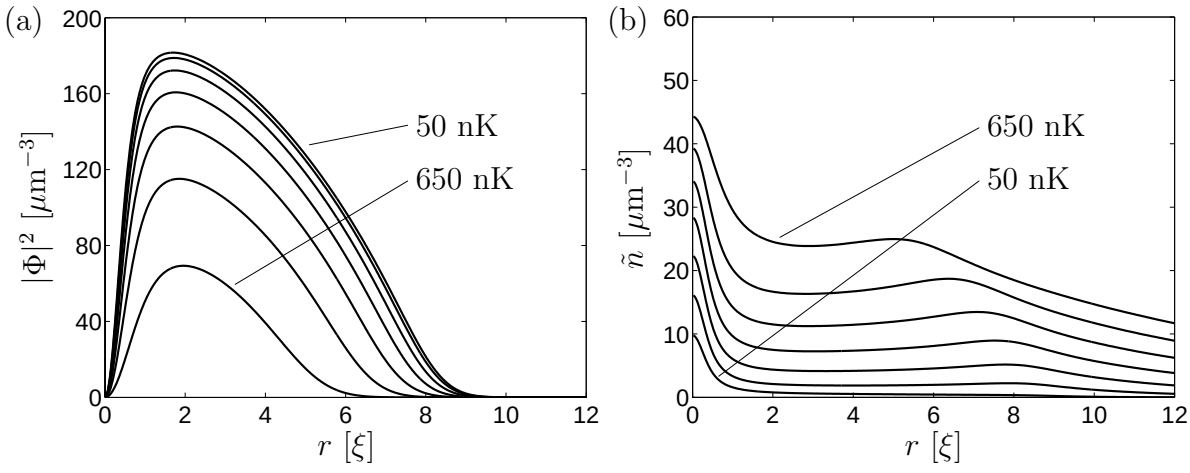

Figure 3.6: Self-consistent density profiles for the condensate (a) and the thermal gas (b) at temperatures $T = 50$, 250, 350, 450, 550 and 650 nK within the PA.

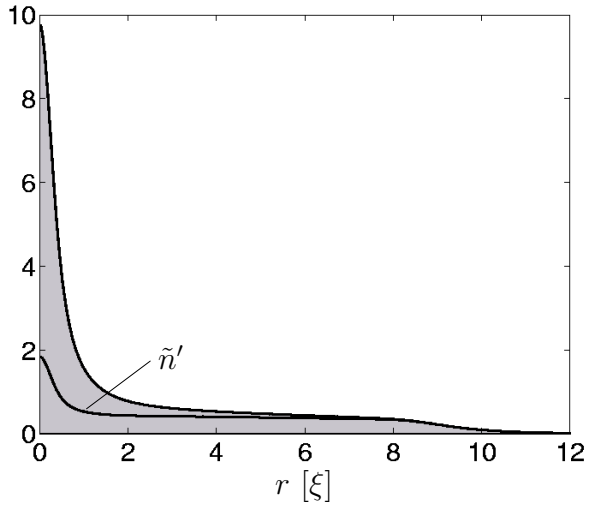

Figure 3.7: The noncondensate density distribution for a cylindrical vortex state at $T = 50$ nK within the PA. The contribution $\tilde{n}'(\mathbf{r})$ from the states other than the LCLS is also shown.

vortex core as a repulsive mean-field potential that lifts the lowest core localized state to positive energies. This lifting effect can be understood by considering the effective potential

$$V_{\text{eff}}(\mathbf{r}) = V_{\text{trap}}(\mathbf{r}) + 2gn(\mathbf{r}) - \mu, \tag{3.21}$$

which appears as a Hartree mean field for quasiparticles in Eqs. (2.27). If the thermal component contribution in the total density $n(\mathbf{r})$ is neglected, V_{eff} is negative in the vortex core region, thus enabling a core localized excitation to have a negative energy. On the other hand, even a small amount of thermal gas concentrated in the core region substantially affects the effective potential felt by the lowest state that is localized into the same region, and lifts its energy owing to the repulsive mean-field interaction. For the specific physical parameter values used, a noncondensate fraction of less than 1% manages to stabilize the vortex in the zero-temperature limit.

In fact, as displayed in Fig. 3.7, at low temperatures the noncondensate peak in the core region originates essentially from the LCLS occupation itself—the energies of the other excitation modes are always of order $E \sim \hbar\omega_\perp$, and their occupations thus negligible for temperatures well below the harmonic trapping energy scale. It is to be noted that the occupation of the LCLS is finite even in the zero-temperature limit since its energy vanishes linearly as the temperature approaches zero. Consequently, it is essentially the repulsive interaction of the LCLS with itself that ultimately lifts its energy to positive values and stabilizes the vortex at low temperatures (see also the analytic argument presented in Ref. [44], p. R176).

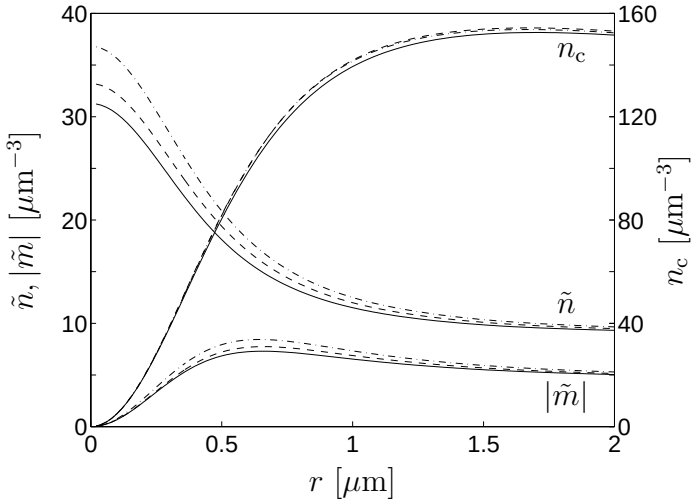

Figure 3.8: Density profiles for the condensate, thermal cloud and the anomalous average in the core region of a cylindrical condensate vortex state within the PA (solid line), the G1 (dashed line) and the G2 (dashed-dotted line) at temperature $T = 400$ nK.

Differences between gapless HFB theories

The differences in the vortex structures between the PA and its G1 and G2 extensions were analysed in Paper II. Previously, corresponding comparisons had been done only for irrotational condensate states [26, 46, 79, 89]. A comparison of these theories for strongly inhomogeneous vortex states is especially interesting since the G1 and G2 extensions are based on assumptions about the momentum dependence of the full many-body T-matrix which can be shown to be valid only in the homogeneous gas limit [46]. Thus, their validity and precision for inhomogeneous states remains to be investigated.

As shown in Paper I, all these gapless HFB formalisms qualitatively agree in predicting the vortex state to be energetically stable at all temperatures below $T_{\rm BEC}$. Also, on the basis of Paper II, the condensate and thermal gas density profiles differ by only a few percent between these theories outside the vortex core region. However, in the core region the differences turn out to be substantial. Fig. 3.8 presents the density profiles of the condensate and the thermal gas in the vicinity of the core region at temperature $T \simeq 0.5 T_{\rm BEC}$. On the vortex axis, the total density is approximately 20% higher in the G2 than in the PA. The higher core density in the G2 can be understood in terms of the "softening" of the repulsive interaction in this region due to many-body effects (cf. Refs. [46, 79]).

The density profiles suggest that differences in the excitation spectra between the approximations are largest for quasiparticle states localized in the vortex core region. Indeed, the LCLS was found to be especially sensitive to the variations in the density. Fig. 3.9 displays the energy of the LCLS as a function of temperature for the PA, G1 and G2. The relative differences between the approximations in the LCLS energy are 25–40%

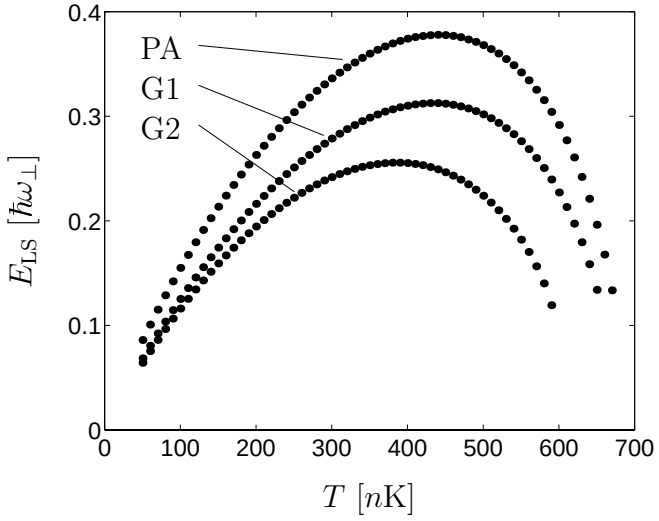

Figure 3.9: The LCLS energy for a cylindrical vortex state as a function of temperature within the PA, G1 and G2.

even at temperatures $T \lesssim 0.6T_{\rm BEC}$, where the PA has excellent precision in describing the spectra of irrotational condensates. For other modes, the differences in the energy were found to be much smaller.

The substantial differences in vortex core density and the LCLS energy were argued to provide stringent tests for the precision of the mean-field theories considered. Especially, such tests were suggested to be valuable in assessing the validity of the G1 and the G2 theories in modelling strongly inhomogeneous systems.

Comparison to experimental results

Due to the diluteness of gaseous BECs, the vortex core diameters in these systems are microscopically large and exceed the corresponding value for ^{4}He by several orders of magnitude. In experimental realizations of condensate vortex states, the healing length essentially determining the core radius has been of order $\xi \simeq 1$ μm, while the core parameter for ^{4}He is $a \simeq 0.8$ Å at atmospheric pressures [30]. Consequently, the vortex structures in alkali-atom condensates are almost visible. By switching off the trap potential and letting the cloud to expand ballistically by a factor of order 10, vortex configurations can actually be imaged [38–43, 117]. Finally, the free expansion process can be modelled theoretically in order to extract precise information on the original condensate state [158–160]. Although the method is destructive, the dynamical evolution of vortices can be followed by a series of such measurements.

The first systematic experimental investigation of vortex dynamics in gaseous BECs was conducted by the JILA group [38]. The vortices were initially created in a nearly spherical two-component condensate confined by a static trap. The irrotational component partly fills the vortex core and, due to repulsive interactions, enlarges it to the degree that the vortex can be observed by using nondestructive phase-contrast imaging.

The irrotational component can be reduced or totally removed with suitable resonant light beams. If completely removed, the core shrinks and the vortex can be observed only using destructive ballistic-expansion imaging.

The vortices were observed to precess in circular orbits with practically constant radii, the precession direction coinciding the direction of the condensate vortex flow.* The negligible radial movement of the vortices implies that dissipation in the system was very weak—the characteristic decay time of vortices at the gas densities used in the experiments substantially exceeds the lifetime of the condensate [156]. The dependence of the precession frequency $\nu_{\rm pr}$ on the radial core displacement and the degree of filling of the core with the irrotational condensate component were also studied. For relative displacements in the range $\zeta = 0.2$–0.4, the frequency $\nu_{\rm pr}$ was found to be almost constant. The precession frequency showed a decreasing trend for increased core filling, but this dependence was rather weak; for core radii of order 10ξ associated with substantial core filling, $\nu_{\rm pr}$ exceeded on the average half the value for bare-core vortices.

The measured bare-core precession frequencies and, especially, the precession directions agree with the predictions of the Bogoliubov approximation—in the precession frequency, the relative difference between the measured and computed values is of order 10% [140]. On the other hand, the observations definitely disagree with the picture given by the PLAs (PA, G1 and G2), which imply precession in the opposite direction at least in the limit of small precession radii. The analysis of this discrepancy resulted in Papers III and IV, the main results of which are presented in the following Subsection.

Effects of noncondensate dynamics

The Popov approximation and its extensions G1 and G2 have been quite successful in modelling the collective modes of irrotational condensates, and the obvious discrepancy between their predictions for the vortex state precession mode and experimental observations is surprising. The mean-field approximation itself seems not to be the cause of this discrepancy, since the Bogoliubov approximation describes the observed vortex dynamics qualitatively correctly, and even quantitatively with reasonably good accuracy.

Essentially, there are three conceivable possibilities to explain this discrepancy: The degree of thermalization of the vortex states in the JILA experiments was incomplete, the motion of off-axis vortices modifies their physics compared to stationary vortex states, or the PLAs simply fail in describing the lowest energy collective modes of vortex states. It is to be noted that dissipation was indeed weak in the JILA conditions, raising doubts that moving vortices were not perfectly thermalized. If the degree of thermalization is low, the LCLS occupation may be negligible and the vortex core not properly filled with the noncondensate. It is to be noted that while thermalization on

*A few counterprecessing vortices were also observed. These "rogue" vortices seemed to have somewhat anomalous structures, and the inverse precession direction was speculated to arise from a complicated distribution of angular momentum between the two condensate components [38].

average may be fast compared to the precession velocity of the vortex, certain degrees of freedom may thermalize much slower than others [161]. However, higher dissipation and thermalization rates in other experiments have resulted in decay of vortices rather than their stabilization [39–43]. Improper thermalization seems thus not to be a probable reason underlying the failure of PLAs to describe the JILA experiments.

In Paper III it is pointed out that the typical precession velocities of off-axis vortices are high enough to give rise to deformation of the vortex core structure and modification of the excitation spectrum from those of static vortices. Consequently, validity of the stationary mean-field theories in modelling off-axis vortex states is questionable. A criterion for the validity of quasi-static formalisms is derived starting from the time-dependent HFB equations (2.21), which in the Popov approximation can be cast into the form

$$i\hbar\frac{\partial}{\partial t}f_q(\mathbf{r},t) = \mathcal{O}(\mathbf{r},t)f_q(\mathbf{r},t), \tag{3.22}$$

where the matrix notation

$$f_q(\mathbf{r},t) = \begin{pmatrix} u_q(\mathbf{r},t) \\ v_q(\mathbf{r},t) \end{pmatrix}, \qquad \mathcal{O}(\mathbf{r},t) = \begin{pmatrix} \mathcal{L}(\mathbf{r},t) & -g\Phi^2(\mathbf{r},t) \\ g\Phi^{*2}(\mathbf{r},t) & -\mathcal{L}(\mathbf{r},t) \end{pmatrix} \tag{3.23}$$

has been used ($\mathcal{L} = \mathcal{L}_{\mathbf{\Omega}=\mathbf{0}}$). If the mean fields vary slowly in time, Eq. (3.22) may be approximated by the quasi-stationary eigenequations

$$E_q(t)f_q^{(0)}(\mathbf{r},t) = \mathcal{O}(\mathbf{r},t)f_q^{(0)}(\mathbf{r},t). \tag{3.24}$$

For this *adiabatic approximation* [162] to be justified, the transition rates between the quasi-stationary states $f_q^{(0)}$ must be negligible in the exact time development of the system. As shown in Paper III, this criterion can be formulated quantitatively with the requirement

$$\left|\frac{1}{\omega_{qq'}}\langle f_{q'}^{(0)}|\dot{f}_q^{(0)}\rangle_{\pm}\right| \ll 1 \qquad \text{(for all } q'\text{)}, \tag{3.25}$$

where the positive- and negative-sign scalar products are defined as

$$\langle f_q|f_{q'}\rangle_{\pm} = \int d\mathbf{r}\,[u_q^*(\mathbf{r})u_{q'}(\mathbf{r}) \pm v_q^*(\mathbf{r})v_{q'}(\mathbf{r})], \tag{3.26}$$

the transition frequency $\omega_{qq'} = (E_q - E_{q'})/\hbar$, and $\dot{f}_q^{(0)}$ denotes the time derivative of $f_q^{(0)}$. The quasiparticle states are normalized according to

$$|\langle f_q^{(0)}|f_q^{(0)}\rangle_{\pm}| = 1, \tag{3.27}$$

where the minus sign is used for states with $\langle f_q^{(0)}|f_q^{(0)}\rangle_- \neq 0$, and the plus sign otherwise—the sign of the scalar product in Eq. (3.25) is chosen according to the normalization of the state $f_{q'}^{(0)}$.

Essentially, this validity criterion shows that the adiabatic approximation is accurate if the kinetic rates in the system are much slower than the frequency separations between

certain excitation levels. Due to the smallness of the characteristic trapping energy scale corresponding to time scales of order $\tau \sim 1/\bar{\omega}_{\rm tr} \sim 1$s, even rather slowly time-dependent phenomena may violate the adiabaticity criterion. Concerning vortex dynamics, it is interesting to find out whether nonadiabatic effects are relevant for precessing vortices. The characteristic kinetic rate for moving vortices is essentially determined by the time in which the vortex traverses a distance corresponding to its core diameter. For circular precession orbits with radii $R_{\rm pr} \gtrsim \xi$, this characteristic kinetic rate exceeds the precession mode frequency. As the latter is typically given by the harmonic trapping frequency, nonadiabatic effects are expected to be relevant for precessing vortices.

A more detailed estimate on the adiabaticity of moving vortices is presented in Paper III.* Considering a circularly precessing vortex line in a cylindrically trapped ($\lambda = 0$) condensate, the matrix element appearing in the criterion (3.25) was estimated by using the uniform vortex motion approximation

$$\langle f^{(0)}_{q'} | \dot{f}^{(0)}_{q} \rangle_{\pm} \simeq \mathbf{v} \cdot \langle f^{(0)}_{q'} | \nabla f^{(0)}_{q} \rangle_{\pm}, \tag{3.28}$$

where $\mathbf{v}$ is the velocity of the vortex line. Equations (3.25) and (3.28) yield for the vortex velocity $\mathbf{v} = |\mathbf{v}|\hat{\mathbf{v}} = v\hat{\mathbf{v}}$ the criterion

$$v \ll v_{qq'} = \left| \frac{\omega_{qq'}}{\hat{\mathbf{v}} \cdot \langle f^{(0)}_{q'} | \nabla f^{(0)}_{q} \rangle_{\pm}} \right| \qquad \text{(for all } q') \tag{3.29}$$

for the quasiparticle state $f^{(0)}_{q}$ to follow the moving vortex adiabatically. The limiting adiabaticity velocities $v_{qq'}$ were estimated by using quasiparticle solutions for an axisymmetric vortex state to approximate the matrix elements. Fig. 3.10 presents these limiting velocities for transitions between the lowest collective modes in the conditions of the JILA experiments [38]. Comparison of the computed adiabaticity velocities to the experimental vortex precession velocity $v_{\rm exp} \simeq 0.1$mm/s reveals the criterion (3.29) to be poorly fulfilled, implying nonadiabatic effects to be nonnegligible. Especially, the slow limiting velocity implied by transitions between the LCLS and the so-called breathing mode is interesting, as the LCLS crucially affects the core structure and the self-stabilization mechanism of the vortex. Deformation of the LCLS would imply substantial modifications to the vortex core structure and possibly also affect the self-stabilization mechanism.

The analysis presented in Paper III shows nonadiabatic effects to be important for precessing off-axis vortices. In order to investigate whether the deformation of the core due to vortex motion could affect the self-stabilization mechanism, uniformly precessing vortices in a staticly trapped, repulsively interacting condensate were investigated in Paper IV using the fully time-dependent Popov approximation introduced in Section 2. In the frame co-rotating with the vortex, the time-dependent Gross-Pitaevskii equation

*A similar analysis on the nonadiabatic effects for moving vortices in superconductors has been presented in Ref. [163].

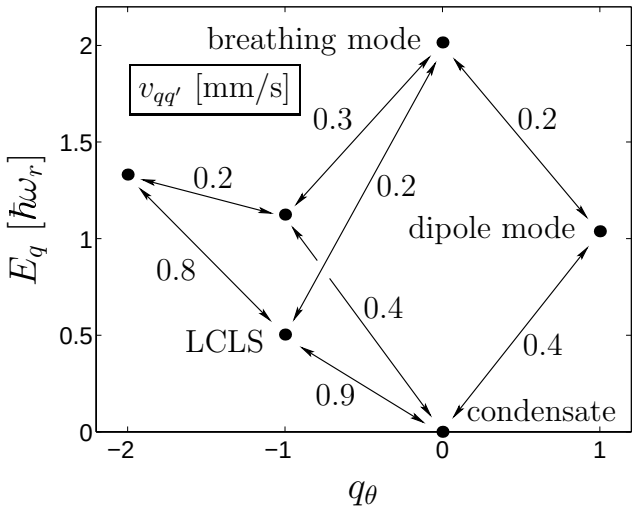

Figure 3.10: The lowest part of the quasiparticle spectrum for a vortex state and the adiabaticity velocities implied by transition rates between the states within the PA at temperature $T \simeq 0.8T_{\rm BEC}$. The parameter values correspond to the JILA experiments. The arrows denote decay channels of the modes to each other, and the numbers are the corresponding adiabaticity velocities $v_{qq'}$ [mm/s].

(2.16) and the quasiparticle equations (2.21) reduce in the Popov approximation to the stationary equations

$$\mathcal{L}_{\mathbf{\Omega}_{\rm pr}}(\mathbf{r})\Phi(\mathbf{r}) - gn_{\rm c}(\mathbf{r})\Phi(\mathbf{r}) = 0, \tag{3.30}$$

for the condensate wave function and

$$\mathcal{L}_{\mathbf{\Omega}_{\rm pr}}(\mathbf{r})u_q(\mathbf{r}) - g\Phi^2(\mathbf{r}) = E'_q u_q(\mathbf{r}), \tag{3.31a}$$

$$\mathcal{L}_{-\mathbf{\Omega}_{\rm pr}}(\mathbf{r})v_q(\mathbf{r}) - g\Phi^{*2}(\mathbf{r}) = -E'_q v_q(\mathbf{r}) \tag{3.31b}$$

for the quasiparticle amplitudes. Above, $\mathbf{\Omega}_{\rm pr}$ is the angular velocity of the precessing vortex. In the course of thermalization, a staticly trapped system approaches the equilibrium statistical distribution determined by its energy spectrum in the laboratory frame of reference. The expectation values $\langle E\rangle$ of quasiparticle energies in the laboratory frame and the eigenenergies E' in the rotating frame are found to be related by

$$\langle E\rangle = E' + \int d\mathbf{r}\ [u^*(\mathbf{\Omega}_{\rm pr}\cdot\mathbf{L})u + v(\mathbf{\Omega}_{\rm pr}\cdot\mathbf{L})v^*] \tag{3.32}$$

for a given quasiparticle eigenstate (E', u, v).

The self-stabilization of vortex states due to the noncondensate was studied by deriving a lower bound for the quasiparticle energies. By neglecting the kinetic energy terms, one obtains for a repulsively interacting gas the lower bound

$$\langle E\rangle > \int d\mathbf{r}\,\rho(V_{\rm trap} + gn_{\rm c} + 2g\tilde{n} - \mu), \tag{3.33}$$

where $\rho = |u|^2 + |v|^2$ is the density distribution of the quasiparticle state. Furthermore, since the lowest states are strongly localized into the vortex core region, it is useful to split the above integral into contributions from the vortex core region C and its complement C'. In terms of the Thomas-Fermi approximation

$$n_{\rm c}^{\rm (TF)} = \frac{1}{g}(\mu - V_{\rm trap} - 2g\tilde{n}) \tag{3.34}$$

for the condensate density and the parameter

$$w = \frac{\int_C d\mathbf{r}\, \rho}{\int_{C'} d\mathbf{r}\, \rho} \tag{3.35}$$

characterizing the degree of quasiparticle core localization, the inequality (3.33) implies

$$\langle E \rangle > \int_C d\mathbf{r}\, \rho \left[V_{\rm trap} + 2g\tilde{n} - \mu - g \max_{C'}\{n_{\rm c}^{\rm (TF)} - n_{\rm c}\}/w \right], \tag{3.36}$$

where $\max_{C'}\{\cdots\}$ denotes the maximum value of its argument outside the vortex core region. For the mode to be anomalous, the integrand has to attain negative values somewhere in the core region, i.e.

$$\tilde{n} < \frac{1}{2g}\left(\mu - V_{\rm trap} + g \max_{C'}\{n_{\rm c}^{\rm (TF)} - n_{\rm c}\}/w \right). \tag{3.37}$$

As argued in Paper IV, the last term on the right-hand side may be neglected for anomalous modes if the gas is sufficiently strongly interacting and the temperature is not too close to $T_{\rm BEC}$. In such a case the inequality (3.37) reduces to

$$\tilde{n}(\mathbf{r}) \lesssim \frac{1}{2} n_0(\mathbf{r}) \tag{3.38}$$

for some $\mathbf{r} \in C$, where n_0 is the local maximum density in the vicinity of the vortex core. This result implies the anomalous modes to be lifted to positive energies as the noncondensate in the core region fills approximately half of the core volume. Moreover, such filling of the core is a natural consequence of thermalization and the existence of the anomalous core modes themselves. The self-stabilization mechanism is thus valid quite generally for the PA and other formalisms sharing the same structure.*

In Paper IV, this stabilization mechanism contradicting the experimental observations and the predictions of the BA is interpreted to originate from the improper treatment of the noncondensate dynamics by the Popov-like approximations. Basically, these approximations treat the noncondensate concentrated in the core region as a static pinning potential for the vortex. The lifting effect for the energies of the core-localized anomalous modes of such a static repulsive potential is naturally stronger than that of a

*The argument presented in Paper IV remains valid also if the orthogonality condition between the condensate and the excited states is imposed. For details, see Ref. [68], p. 3857.

realistic, dynamical noncondensate peak. The improper treatment of the noncondensate dynamics is also reflected to the LCLS, which in the PA describes precession of the vortex about a static noncondensate peak rather than a coupled motion of them (see also the discussion in Ref. [44], p. R177). In conclusion, a reliable analysis of the stability and dynamics of condensate vortex states requires a formalism that takes properly into account the coupled dynamics of the condensate and the noncondensate.

3.4 Stabilization of multiquantum vortices

Multiply quantized vortices (MQVs) are known to be energetically unstable in homogeneous superfluids described by a scalar order parameter [30]. Basically, this is due to the proportionality of the vortex energy to the square of its circulation, implying splitting of multiply charged vortices to simply quantized ones to be energetically favourable. The conclusion remains valid also when the interaction of vortices in taken into account.

Such vortices can, however, be stabilized by breaking the homogeneity of the superfluid with suitable external potentials. In superconductors, holes, antidots and columnar defects in the underlying atomic lattices have been used as pinning potentials to stabilize MQVs [164–166]. Multicharged vortices have been also observed in thin superconducting films [167] and thin layers of superfluid ^{4}He [168]. Furthermore, such structures exist in bulk superfluid ^{3}He, which has a complicated non-scalar order parameter due to spin degrees of freedom [31].

Harmonically trapped BECs are not homogeneous, but such trapping turns out to be too shallow to allow the existence of stable MQVs in single-component systems. The instability of multiquantum vortices is manifested in the existence of negative energy and complex frequency modes in their excitation spectra. In the 2D cylindrical geometry corresponding to $\lambda = 0$ (cf. Eq. (3.12)), axisymmetric multiquantum vortex states exhibit complex frequency modes corresponding to a splitting instability for certain values of the interaction strength gN [128]. In finite geometries corresponding to $\lambda > 0$, complex frequency splitting modes always exist [169]. In harmonically trapped condensates MQVs are thus not only energetically [97,98,105,139] but also dynamically unstable, and decay even in the absence of dissipation.* Such vortices have recently been, however, created by using topological phase engineering methods [118–120].

One possibility to stabilize MQVs in dilute condensates is to use steeper than harmonic trapping potentials—for example power-law potentials of the form $V_{\rm trap} \sim r^\alpha$ with $\alpha > 2$ provide strong enough confinement to suppress the unstable multiquantum vortex modes for weakly enough interacting condensates [171]. Another way is to use strong enough pinning potentials for vortices. An axisymmetric trap supplemented by a strongly repulsive pinning potential at the symmetry axis essentially corresponds to a toroidal geometry, which supports also multiquantum vortices if the pinning potential

*It is interesting to note that these complex frequency modes are absent for homogeneous ($V_{\rm trap} = 0$) condensates, i.e. the dynamical instability is induced by the trap potential [170].

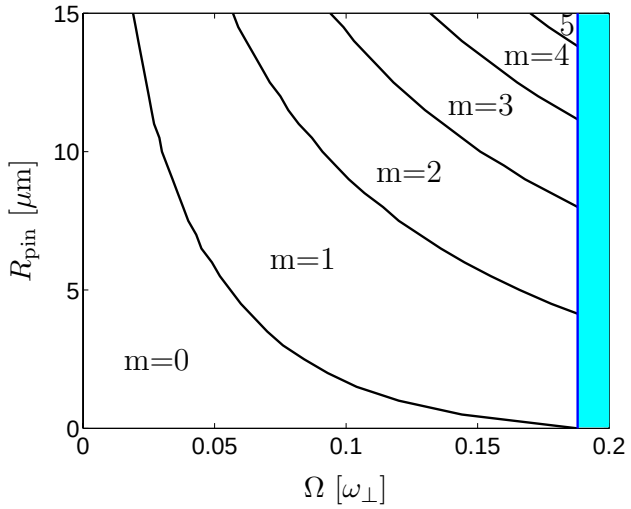

Figure 3.11: Phase diagram for the lowest-energy vortex state as a function of the trap rotation frequency and the radius of the pinning potential. For physical parameter values used, see Paper V.

is thick enough. The additional potential could be realized by focusing a blue-detuned laser beam through the trap center.

In Paper V, conditions for energetically stabilizing multiquantum vortices in such a cylindrical geometry are investigated within the Bogoliubov approximation. Energetically favourable states are surveyed with respect to the trap rotation velocity Ω and the radius of the pinning potential $R_{\rm pin}$. For simplicity, the investigation is confined to region $\Omega < \Omega_{\rm c}$, where $\Omega_{\rm c}$ denotes the critical rotation velocity at which the singly quantized axisymmetrix vortex states becomes energetically favourable compared to the irrotational condensate state. In this region one may restrict to consider only axisymmetric vortex states.

By computing the vortex state energies as functions of Ω, $R_{\rm pin}$ and the circulation quantum number m, the phase diagram represented in Fig. 3.11 was obtained. The diagram displays the minimum energy state in the $\Omega R_{\rm pin}$ plane, and shows that MQVs can indeed be made energetically favourable in rotating traps with suitable pinning potentials. In addition, the pinning potentials rendering a given number of circulation quanta energetically favourable are also shown to locally energetically stabilize the corresponding vortex state. Consequently, it is suggested to be possible to drive the system continuously into a multiquantum state by starting from a configuration containing only singly quantized vortices.

4 Numerical Methods for Solving BdG Equations

The Hartree-Fock-Bogoliubov (HFB) equations, i.e. the quasiparticle eigenequations (2.27) supplemented by the self-consistency relations (2.28) result from the quadratic mean-field approximation for a weakly interacting, partially condensed boson gas. Their similar fermionic counterpart, the Bogoliubov-de Gennes (BdG) equations, are of central importance in the context of superconductivity, where they constitute the wave function formulation of the Bardeen-Cooper-Schrieffer (BCS) theory.*

These quadratic mean-field theories can be solved rather easily for homogeneous systems [73], but for inhomogeneous problems they typically pose serious computational challenges. Although wave function formalisms are natural frameworks in treating inhomogeneous systems, such challenges are expected when trying to extract detailed information on interacting many-particle systems using first-principles quantum theories. In wave function formalisms, these difficulties are manifested in the large number of quasiparticle eigensolutions needed in the self-consistency relations.

An important part of the research summarized in this thesis is the development of computational methods for solving the HFB and BdG equations self-consistently. The computational scheme which enabled finding the previously inaccessible low-temperature vortex solutions presented in Papers I and II was initially developed for fermionic BdG equations. In Subsection 4.1, this computational scheme is presented in the context of the BCS theory of superconductivity, and compared to other methods commonly used. This is also the subject of Papers VI–VIII. Finally, in Subsection 4.2, the specific computational features of bosonic HFB equations are discussed.

4.1 Fermionic systems

The Bogoliubov-de Gennes equations of superconductivity consist of the coupled eigenvalue equations

$$\mathcal{H}_e(\mathbf{r})u_q(\mathbf{r}) + \int d\mathbf{r}'\, \Delta(\mathbf{r},\mathbf{r}')v_q(\mathbf{r}) = E_q u_q(\mathbf{r}), \tag{4.1a}$$

$$-\mathcal{H}_e^*(\mathbf{r})v_q(\mathbf{r}) + \int d\mathbf{r}'\, \Delta^*(\mathbf{r},\mathbf{r}')u_q(\mathbf{r}) = E_q v_q(\mathbf{r}) \tag{4.1b}$$

for the quasiparticle energies E_q and amplitudes $u_q(\mathbf{r})$, $v_q(\mathbf{r})$ [172]. Above, $\mathcal{H}_e(\mathbf{r})$ denotes the single-electron Hamiltonian

$$\mathcal{H}_e(\mathbf{r}) = -\frac{\hbar^2}{2m_e}\left[\nabla - \frac{ie}{\hbar c}\mathbf{A}(\mathbf{r})\right]^2 + U_0(\mathbf{r}) - E_\mathrm{F}, \tag{4.2}$$

where $\mathbf{A}(\mathbf{r})$ is the magnetic field vector potential, $U_0(\mathbf{r})$ the external lattice potential and E_F the Fermi energy of electrons. The BdG equations are coupled integro-differential

*The HFB quasiparticle equations (2.27) are also sometimes called Bogoliubov-de Gennes equations.

equations if the pairing potential $\Delta(\mathbf{r},\mathbf{r}')$ is nonlocal. They are furthermore supplemented by the self-consistency conditions relating the pairing amplitude and the current density $\mathbf{j}(\mathbf{r})$ to the quasiparticle eigensolutions:

$$\Delta(\mathbf{r},\mathbf{r}') = V(\mathbf{r},\mathbf{r}')\sum_q [1-2f(E_q)][v_q^*(\mathbf{r})u_q(\mathbf{r}')+v_q^*(\mathbf{r}')u_q(\mathbf{r})], \tag{4.3a}$$

$$\begin{aligned}\mathbf{j}(\mathbf{r}) = \frac{e\hbar}{m_e}\sum_q \mathrm{Im}\Bigg\{ & f(E_q)u_q^*(\mathbf{r})\left[\nabla - \frac{ie}{\hbar c}\mathbf{A}(\mathbf{r})\right]u_q(\mathbf{r}) \\ & + [1-f(E_q)]v_q(\mathbf{r})\left[\nabla - \frac{ie}{\hbar c}\mathbf{A}(\mathbf{r})\right]v_q^*(\mathbf{r})\Bigg\},\end{aligned} \tag{4.3b}$$

where $V(\mathbf{r},\mathbf{r}')$ describes the electronic pairing interaction and $f(E_q) = (e^{E_q/k_\mathrm{B}T}+1)^{-1}$ is the Fermi-Dirac distribution function. The summations in the self-consistency relations include all states below a suitable cut-off energy.

Finding self-consistent solutions to the BdG equations is computationally demanding. The number of quasiparticle eigenstates required in the self-consistency summations scales as $\sim L^3$ with respect to a characteristic system dimension L, and is large even for $L \simeq \xi$, where ξ is the superconducting coherence length characterizing spatial variations in the pairing amplitude. Another major computational challenge is hidden in the two widely separated length scales of the problem: The coherence length scale often substantially exceeds the Fermi length scale that characterizes the oscillations in the quasiparticle amplitudes. In addition, the nonlocality of the pairing amplitude, albeit usually of short range, is a challenge for finding efficient computational methods for the quasiparticle equations. In practice, 3D problems are overwhelmingly time-consuming to solve self-consistently even with modern supercomputers. Fortunately, many interesting problems have continuous spatial symmetries, which can be utilized to reduce the effective computational dimensionality. The first effectively 2D problems are becoming computationally feasible, but even for 1D problems one is still restricted to use small computational domains.

In Papers VI–VIII, an efficient computational scheme for solving the BdG equations in effectively 1D geometries is presented. The method is applied to compute electronic structures of isolated multiquantum vortices (Paper VII) and the ultralow-temperature thermodynamics of a superconducting π-junction (Paper VIII).

Similar problems have previously been approached by using typically so-called *eigenfunction expansion methods* (EEMs) [133, 155, 173–175], in which the eigenvalue equations (4.1) are discretized in a function basis typically consisting of eigensolutions in the analytically solvable case $\mathbf{A} = \Delta = U_0 = 0$. The full solutions are approximated by their projections to a subspace spanned by a finite number N of basis functions. The projection converts the eigenequations to an eigenvalue problem of a dense $2N \times 2N$ matrix, which is solved numerically. As argued in Paper VI, the CPU time τ scales for the method as $\tau \sim L^3$, where L is the length of the effectively 1D system.

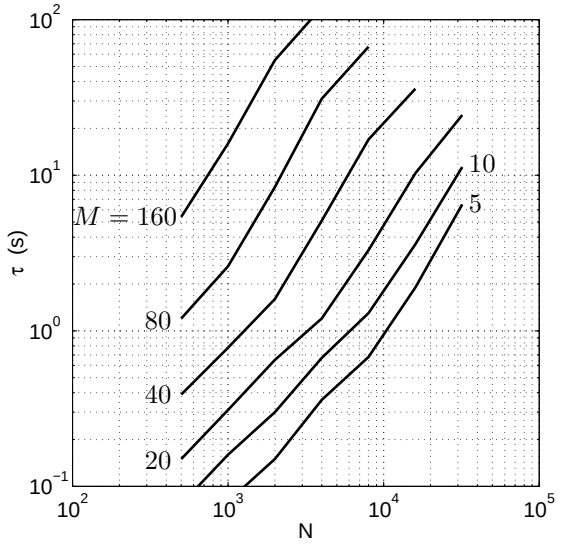

Figure 4.1: The CPU time τ required to compute M lowest eigenstates using the real-space discretization scheme with lattice size N. Compaq AlphaServer GS140 computer and the Lanczos method implemented in ARPACK subroutine libraries have been used in the test. The slight irregularities in τ are due to varying total load of the system.

Instead of an EEM, a scheme based on high-order real-space discretization combined with an iterative Lanczos method eigensolver was used in Papers VII, VIII and Ref. [176]. By using an evenly spaced discretization lattice with N grid points and n-point central-difference formulas to approximate the derivatives, the BdG equations are again transformed to an eigenproblem of a symmetric $2N \times 2N$ matrix. However, this coefficient matrix is now a band matrix with bandwidth $2n-1$ if the pairing amplitude is local, and only slightly wider for typical nonlocal pairing amplitudes.* Although in the real-space discretization the number of degrees of freedom typically has to be larger than that in the EEMs to obtain the same accuracy, the banded structure of the coefficient matrix is a definite advantage with respect to memory storage and CPU time requirements. Furthermore, the real-space discretization allows taking nonlocal short-range pairing amplitudes into account essentially without additional computational cost, in contrast to EEMs.

The narrow-bandedness of the coefficient matrix and the restriction to consider only states up to a given cut-off energy can be fully utilized by using the iterative Lanczos method to solve the discretized eigenvalue problem. Specifically, its implementation in the ARPACK† subroutine libraries was used in Papers VII and VIII. Fig. 4.1 presents the scaling of the CPU time τ of the algorithm as a function of the lattice size N and

*The optimal value for n is approximately 10, while N is typically of order 1000.

†http://www.caam.rice.edu/software/ARPACK/.

the computed number of eigenstates M. The CPU time is seen to scale approximately as $\tau \sim N^{1.5}$, which is substantially more favourable than within the EEMs. The method is thus superior if solutions with high accuracy are required. In Paper VI, the CPU time requirement is shown to scale as $\tau \sim L^{2.5}$ as a function of the system size for a fixed discretization lattice density. This scaling is also advantageous compared to the EEMs with $\tau \sim L^3$, and enables using larger computational domains.

4.2 Bosonic systems

The bosonic HFB equations closely resemble the fermionic BdG equations, suggesting similar computational methods to be applicable in solving them. However, there exists also crucial differences between these formalisms: The fermionic quasiparticle Hamiltonian

$$\mathcal{H}_{\mathrm{BdG}} = \begin{pmatrix} \mathcal{H}_e(\mathbf{r}) & \Delta(\mathbf{r},\mathbf{r}') \\ \Delta^*(\mathbf{r},\mathbf{r}') & -\mathcal{H}_e^*(\mathbf{r}) \end{pmatrix} \tag{4.4}$$

is Hermitian at least for local pairing amplitudes, while the HFB Hamiltonian

$$\mathcal{H}_{\mathrm{HFB}} = \begin{pmatrix} \mathcal{L}(\mathbf{r}) & -g\Phi^2(\mathbf{r}) \\ g\Phi^{*2}(\mathbf{r}) & -\mathcal{L}(\mathbf{r}) \end{pmatrix} \tag{4.5}$$

is not. On the other hand, the bosonic equations do not contain such widely separated length scales as the Fermi wavelength and the coherence length for the BdG equations.

Despite these differences, the finite-difference scheme described above can be applied to solve effectively the HFB equations with only slight modifications [177]. Due to the absence of short-wavelength oscillations in the bosonic quasiparticle amplitudes, the discretization grid can be chosen relatively much sparcer than in the case of fermionic BdG equations. Instead of the Lanczos method, the nonhermiticity of $\mathcal{H}_{\mathrm{HFB}}$ requires using the more general Arnoldi method in solving the discretized eigenvalue problem. This does not, however, essentially affect the scaling behaviour of the CPU time requirement.

5 Summary

The main objective of the research presented in this thesis was to investigate quantized vortices in dilute atomic Bose-Einstein condensates within microscopic finite-temperature mean-field theories.

In Papers I and II, the structure and stability of vortices in partially condensed atomic vapours were investigated using the self-consistent Popov approximation and its gapless extensions G1 and G2. Substantial structural differences in the vortex core region were found between the formalisms. However, quite surprisingly, the energetically unstable pure-condensate vortex states were found to be stabilized by the noncondensed gas component even in the zero-temperature limit within all these Popov-like approximations.

The analysis of this self-stabilization mechanism and the related problem of vortex precession direction lead to results presented in Papers III and IV. In Paper III, it was argued that under typical experimental conditions the deformation of quasiparticle excitations due to nonadiabatic effects should be taken into account when modelling time-dependent condensate states at finite temperatures. Especially, the thermal cloud was shown to be unable to follow precessing off-axis vortices rigidly, giving rise to deformation of the core structure of moving vortices. Fully time-dependent quasiparticle equations should thus be used to correctly model such states, instead of the (quasi)stationary equations corresponding to the adiabatic approximation. The failure of the adiabatic approximation also compromises the prediction of energetic stability of vortex states given by the stationary Popov-like formalisms.

In order to find out whether the core deformation could affect the stability of moving vortices, in Paper IV uniformly precessing off-axis vortex states were analysed using a fully time-dependent Popov approximation. A lower bound was derived for the quasiparticle energies, showing that a partial filling of the vortex core with noncondensed gas always suffices to lift the energies of unstable anomalous modes to positive values, thus rendering vortex states energetically metastable. Furthermore, such filling of the core region is a natural consequence of thermalization and the existence of core-localized anomalous modes themselves. The results presented in Paper I showing axisymmetric vortex states to be metastable within the Popov approximation were thus argued to be valid also for general off-axis vortex states.

The unphysical prediction of vortex stability was argued to originate from the improper treatment of the noncondensate dynamics inherent for first-order mean-field approximations. This defect of the Popov-like formalisms has been attributed to their failure in predicting the excitation spectra of irrotational condensates near T_{BEC}, but its relevance also in the low-temperature limit has not been recognized previously.

Stabilization of multiquantum vortex states in harmonically trapped condensates by using an additional repulsive pinning potential was investigated in Paper V. The phase diagram for energetically favourable vortex states as function of the trap rotation velocity and the width of the pinning potential was presented. The pinning potentials

required to render multiquantum vortices energetically favourable were also shown to locally energetically stabilize the corresponding vortex states.

The computational methods facilitating the survey of self-consistent vortex solutions in the zero-temperature limit were initially developed for the fermionic Bogoliubov-de Gennes equations used to model inhomogeneous superconductors. The numerical scheme was presented in Papers VI–VIII with applications to multiquantum vortex states and π-junctions in s-wave superconductors. As functions of the system size and numerical accuracy, the scaling of the CPU time and memory storage requirements of the method were shown to be preferable compared to other methods commonly used. In addition, short-range nonlocal pairing interactions can be taken into account in the scheme without essentially increasing the computational cost.

During the recent years, the experimental breakthroughs in creating and manipulating alkali-atom condensates have also invigorated the development of thermal field theories for weakly interacting BECs. The success of lowest-order mean-field theories in modelling these systems has been remarkable, but the rapid development in experimental methods is beginning to provide measurement data accurate enough to pose definite tests for theories taking into account higher-order effects. Due to strong inhomogeneities, vortex states are especially suitable for testing the validity of theoretical models. The results presented in this thesis indicate that the most common finite-temperature mean-field theories used to model dilute atomic BECs drastically fail when applied to vortex states. This failure underlines the need for a computationally feasible finite-temperature formalism that consistently extends beyond the Popov approximation in taking into account higher-order atomic correlations and in treating the dynamics of the condensed and noncondensed components on an equal footing.

References

[1] S. Bose, Z. Phys. **26**, 178 (1924).

[2] A. Einstein, Sitzungber. Kgl. Preuss. Akad. Wiss. **1924**, 261 (1924).

[3] A. Einstein, Sitzungber. Kgl. Preuss. Akad. Wiss. **1925**, 3 (1925).

[4] F. London, Nature **141**, 643 (1938).

[5] P. Sokol, in *Bose-Einstein Condensation*, edited by A. Griffin, D. W. Snoke, and S. Stringari (Cambridge University Press, Cambridge, 1995), Chap. 4, pp. 51–85.

[6] D. M. Ceperley, Rev. Mod. Phys. **67**, 279 (1995).

[7] J. Bardeen, L. N. Cooper, and J. R. Schrieffer, Phys. Rev. **108**, 1175 (1957).

[8] *Bose-Einstein Condensation*, edited by A. Griffin, D. W. Snoke, and S. Stringari (Cambridge University Press, Cambridge, 1995).

[9] M. H. Anderson *et al.*, Science **269**, 198 (1995).

[10] K. B. Davis *et al.*, Phys. Rev. Lett. **75**, 3969 (1995).

[11] C. C. Bradley, C. A. Sackett, J. J. Tollett, and R. G. Hulet, Phys. Rev. Lett. **75**, 1687 (1995), *ibid.* **79**, 1170 (1997).

[12] K. Burnett, in *Proceedings of the International School of Physics - Enrico Fermi*, edited by M. Inguscio, S. Stringari, and C. E. Wieman (IOS Press, Amsterdam, 1999), p. 265.

[13] Ph. W. Courteille, V. S. Bagnato, and V. I. Yukalov, Laser Phys. **11**, 659 (2001).

[14] M. Le Bellac, *Thermal Field Theory* (Cambridge University Press, Cambridge, 1996).

[15] M.-O. Mewes *et al.*, Phys. Rev. Lett. **78**, 582 (1997).

[16] M. Greiner *et al.*, Nature **415**, 39 (2002).

[17] J. R. Anglin and W. H. Zurek, Phys. Rev. Lett. **83**, 1707 (1999).

[18] U. Leonhardt and P. Piwnicki, Phys. Rev. Lett. **84**, 822 (2000).

[19] D. O'Dell, S. Giovanazzi, G. Kurizki, and V. M. Akulin, Phys. Rev. Lett. **84**, 5687 (2000).

[20] N. N. Bogoliubov, J. Phys. (Moscow) **11**, 23 (1947).

[21] A. L. Fetter, Ann. Phys. (N. Y.) **70**, 67 (1972).

[22] F. Dalfovo, S. Giorgini, L. P. Pitaevskii, and S. Stringari, Rev. Mod. Phys. **71**, 463 (1999).

[23] V. N. Popov, in *Functional Integrals and Collective Modes* (Cambridge University Press, New York, 1987), Chap. 6.

[24] A. Griffin, Phys. Rev. B **53**, 9341 (1996).

[25] R. J. Dodd, M. Edwards, C. W. Clark, and K. Burnett, Phys. Rev. A **57**, R32 (1998).

[26] D. A. W. Hutchinson *et al.*, J. Phys. B: At. Mol. Opt. Phys. **33**, 3825 (2000).

[27] D. R. Tilley and J. Tilley, *Superfluidity and Superconductivity* (Hilger, Bristol, 1986).

[28] P. W. Anderson, Rev. Mod. Phys. **38**, 298 (1966).

[29] A. J. Leggett, in *Bose-Einstein Condensation*, edited by A. Griffin, D. W. Snoke, and S. Stringari (Cambridge University Press, Cambridge, 1995), Chap. 19, p. 452.

[30] R. J. Donnelly, *Quantized Vortices in Helium II* (Cambridge University Press, Cambridge, 1991).

[31] D. Vollhardt and P. Wölfle, *The Superfluid Phases of Helium 3* (Taylor and Francis, London, 1990).

[32] *Superconductivity*, edited by R. D. Parks (Marcel Dekker, New York, 1969).

[33] A. Vilenkin and E. P. S. Shellard, *Cosmic Strings and Other Topological Defects* (Cambridge University Press, Cambridge, 1994).

[34] P. W. Anderson and N. Itoh, Nature **256**, 25 (1975).

[35] G. N. Fowler, S. Raha, and R. M. Weiner, Phys. Rev. C **31**, 1515 (1985).

[36] G. A. Swartzlander, Jr. and C. T. Law, Phys. Rev. Lett. **69**, 2503 (1992).

[37] M. R. Matthews *et al.*, Phys. Rev. Lett. **83**, 2498 (1999).

[38] B. P. Anderson, P. C. Haljan, C. E. Wieman, and E. A. Cornell, Phys. Rev. Lett. **85**, 2857 (2000).

[39] K. W. Madison, F. Chevy, W. Wohlleben, and J. Dalibard, Phys. Rev. Lett. **84**, 806 (2000).

[40] K. W. Madison, F. Chevy, W. Wohlleben, and J. Dalibard, J. Mod. Opt. **47**, 2715 (2000).

[41] J. R. Abo-Shaeer, C. Raman, J. M. Vogels, and W. Ketterle, Science **292**, 476 (2001).

[42] C. Raman *et al.*, Phys. Rev. Lett. **87**, 210402 (2001).

[43] P. Rosenbusch, V. Bretin, and J. Dalibard, Phys. Rev. Lett. **89**, 200403 (2002).

[44] A. L. Fetter and A. A. Svidzinsky, J. Phys.: Condens. Matter **13**, R135 (2001).

[45] M. Bijlsma and H. T. C. Stoof, Phys. Rev. A **55**, 498 (1997).

[46] N. P. Proukakis, S. A. Morgan, S. Choi, and K. Burnett, Phys. Rev. A **58**, 2435 (1998).

[47] H. Shi and A. Griffin, Phys. Rep. **304**, 1 (1998).

[48] D. J. Heinzen, in *Proceedings of the International School of Physics - Enrico Fermi*, edited by M. Inguscio, S. Stringari, and C. E. Wieman (IOS Press, Amsterdam, 1999), p. 351.

[49] J. Weiner, V. S. Bagnato, S. Zilio, and P. S. Julienne, Rev. Mod. Phys. **71**, 1 (1999).

[50] J. Dalibard, in *Proceedings of the International School of Physics - Enrico Fermi*, edited by M. Inguscio, S. Stringari, and C. E. Wieman (IOS Press, Amsterdam, 1999), p. 321.

[51] E. A. Cornell, J. R. Ensher, and C. E. Wieman, in *Proceedings of the International School of Physics - Enrico Fermi*, edited by M. Inguscio, S. Stringari, and C. E. Wieman (IOS Press, Amsterdam, 1999), p. 15.

[52] W. Ketterle, D. S. Durfee, and D. M. Stamper-Kurn, in *Proceedings of the International School of Physics - Enrico Fermi*, edited by M. Inguscio, S. Stringari, and C. E. Wieman (IOS Press, Amsterdam, 1999), p. 67.

[53] C. J. Pethick and H. Smith, *Bose-Einstein Condensation in Dilute Gases* (Cambridge University Press, Cambridge, 2002).

[54] L. D. Landau and E. M. Lifshitz, *Statistical Physics*, 3rd ed. (Pergamon Press, Oxford, 1980).

[55] A. G. Truscott *et al.*, Science **291**, 2570 (2001).

[56] G. Breit and I. I. Rabi, Phys. Rev. **38**, 2082 (1931).

[57] W. H. Wing, Prog. Quantum Electron. **8**, 181 (1984).

[58] W. Ketterle and D. E. Pritchard, Appl. Phys. B **54**, 403 (1992).

[59] C. Cohen-Tannoudji, in *Fundamental Processes in Quantum Optics*, edited by J. Dalibard, J.-M. Raimond, and J. Zinn-Justin (North-Holland, Amsterdam, 1992), p. 1.

[60] K. Helmerson and W. D. Phillips, in *Proceedings of the International School of Physics - Enrico Fermi*, edited by M. Inguscio, S. Stringari, and C. E. Wieman (IOS Press, Amsterdam, 1999), p. 391.

[61] L. D. Landau and E. M. Lifshitz, *Quantum Mechanics - Non-relativistic Theory* (Pergamon Press, Oxford, 1977).

[62] C. J. Joachain, *Quantum Collision Theory* (North Holland, Amsterdam, 1983).

[63] D. J. Friend and R. D. Etters, J. Low Temp. Phys. **39**, 409 (1980).

[64] E. Tiesinga, B. J. Verhaar, and H. T. C. Stoof, Phys. Rev. A **47**, 4114 (1993).

[65] S. Inouye *et al.*, Nature **392**, 151 (1998).

[66] Ph. Courteille *et al.*, Phys. Rev. Lett. **81**, 69 (1998).

[67] K. Huang, *Statistical Mechanics*, 2nd ed. (Wiley, New York, 1987).

[68] S. Morgan, J. Phys. B: At. Mol. Opt. Phys. **33**, 3847 (2000).

[69] Y. Castin and R. Dum, Phys. Rev. A **57**, 3008 (1998).

[70] C. W. Gardiner, Phys. Rev. A **56**, 1414 (1997).

[71] A. S. Parkins and D. F. Walls, Phys. Rep. **303**, 1 (1998).

[72] N. P. Proukakis and K. Burnett, J. Res. Natl. Inst. Stand. Tech. **101**, 457 (1996).

[73] A. L. Fetter and J. D. Walecka, *Quantum Theory of Many-Particle Systems* (McGraw-Hill, New York, 1971).

[74] E. P. Gross, Nuovo Cimento **20**, 454 (1961).

[75] E. P. Gross, J. Math. Phys. **4**, 195 (1963).

[76] L. P. Pitaevskii, Zh. Éksp. Teor. Fiz. **40**, 646 (1961), [Sov. Phys. JETP **13**, 451 (1961)].

[77] A. S. Alexandrov and W. H. Beere, Phys. Rev. B **51**, 5887 (1995).

[78] S. Giorgini, Phys. Rev. A **57**, 2949 (1998).

[79] T. Bergeman, D. L. Feder, N. L. Balazs, and B. I. Schneider, Phys. Rev. A **61**, 063605 (2000).

[80] N. M. Hugenholtz and D. Pines, Phys. Rev. **116**, 489 (1959).

[81] J. Goldstone, Nuovo Cimento **19**, 154 (1961).

[82] D. A. W. Hutchinson, E. Zaremba, and A. Griffin, Phys. Rev. Lett. **78**, 1842 (1997).

[83] S. T. Beliaev, Zh. Éksp. Teor. Fiz. **34**, 417 (1958), [Sov. Phys. JETP **7**, 289 (1958)].

[84] S. T. Beliaev, Zh. Éksp. Teor. Fiz. **34**, 433 (1958), [Sov. Phys. JETP **7**, 299 (1958)].

[85] K. Huang and C. N. Yang, Phys. Rev. **105**, 767 (1957).

[86] T. D. Lee, K. Huang, and C. N. Yang, Phys. Rev. **106**, 1135 (1957).

[87] T. D. Lee and C. N. Yang, Phys. Rev. **112**, 1419 (1958).

[88] P. O. Fedichev and G. V. Shlyapnikov, Phys. Rev. A **58**, 3146 (1998).

[89] D. A. W. Hutchinson, R. J. Dodd, and K. Burnett, Phys. Rev. Lett. **81**, 2198 (1998).

[90] A. J. Leggett, Rev. Mod. Phys. **71**, S318 (1999).

[91] S.-K. Yip, Phys. Rev. Lett. **83**, 4677 (1999).

[92] T. Isoshima, K. Machida, and T. Ohmi, J. Phys. Soc. Jpn. **70**, 1604 (2001).

[93] T. Isoshima and K. Machida, Phys. Rev. A **66**, 023602 (2002).

[94] A. J. Leggett, Rev. Mod. Phys. **73**, 307 (2001).

[95] F. Dalfovo and S. Stringari, Phys. Rev. A **53**, 2477 (1996).

[96] M. Edwards *et al.*, Phys. Rev. A **53**, R1950 (1996).

[97] D. A. Butts and D. S. Rokhsar, Nature **397**, 327 (1999).

[98] Y. Castin and R. Dum, Euro. Phys. J. D **7**, 399 (1999).

[99] D. L. Feder, C. W. Clark, and B. I. Schneider, Phys. Rev. A **61**, 011601R (1999).

[100] J. J. García-Ripoll and V. M. Pérez-García, Phys. Rev. A **64**, 053611 (2001).

[101] R. S. MacKay, in *Hamiltonian Dynamical Systems*, edited by R. S. Kay and J. D. Meiss (Hilger, Bristol, 1987).

[102] N. K. Wilkin, J. M. F. Gunn, and R. A. Smith, Phys. Rev. Lett. **80**, 2265 (1998).

[103] B. Mottelson, Phys. Rev. Lett. **83**, 2695 (1999).

[104] G. F. Bertsch and T. Papenbrock, Phys. Rev. Lett. **83**, 5412 (1999).

[105] G. M. Kavoulakis, B. Mottelson, and C. J. Pethick, Phys. Rev. A **62**, 063605 (2000).

[106] G. Baym, in *Mathematical Methods in Solid State and Superfluid Theory*, edited by R. C. Clark and G. H. Derrick (Oliver & Boyd, Edinburgh, 1969), Chap. 3.

[107] J. J. García-Ripoll, G. Molina-Terriza, V. M. Pérez-García, and L. Torner, Phys. Rev. Lett. **87**, 140403 (2001).

[108] D. S. Rokhsar, cond-mat/9709212.

[109] M. Benakli *et al.*, cond-mat/9711295.

[110] L. Salasnich, A. Parola, and L. Reatto, Phys. Rev. A **59**, 2990 (1999).

[111] D. S. Rokhsar, Phys. Rev. Lett. **79**, 2164 (1997).

[112] J. E. Williams and M. J. Holland, Nature **401**, 568 (1999).

[113] S. Inouye *et al.*, Phys. Rev. Lett. **87**, 080402 (2001).

[114] B. P. Anderson *et al.*, Phys. Rev. Lett. **86**, 2926 (2001).

[115] Z. Dutton, M. Budde, C. Slowe, and L. V. Hau, Science **293**, 663 (2001).

[116] P. C. Haljan, I. Coddington, P. Engels, and E. A. Cornell, Phys. Rev. Lett. **87**, 210403 (2001).

[117] E. Hodby *et al.*, Phys. Rev. Lett. **88**, 010405 (2002).

[118] A. E. Leanhardt *et al.*, Phys. Rev. Lett. **89**, 190403 (2002).

[119] M. Nakahara *et al.*, Physica B **284–288**, 17 (2000).

[120] T. Isoshima, M. Nakahara, T. Ohmi, and K. Machida, Phys. Rev. A **61**, 063610 (2000).

[121] F. Chevy, K. W. Madison, and J. Dalibard, Phys. Rev. Lett. **85**, 2223 (2000).

[122] K. W. Madison, F. Chevy, V. Bretin, and J. Dalibard, Phys. Rev. Lett. **86**, 4443 (2001).

[123] D. Guéry-Odelin and S. Stringari, Phys. Rev. Lett. **83**, 4452 (1999).

[124] O. M. Maragó *et al.*, Phys. Rev. Lett. **84**, 2056 (2000).

[125] C. Raman *et al.*, Phys. Rev. Lett. **83**, 2502 (1999).

[126] R. Onofrio *et al.*, Phys. Rev. Lett. **85**, 2228 (2000).

[127] S. Burger *et al.*, Phys. Rev. Lett. **86**, 4447 (2001).

[128] H. Pu, C. K. Law, J. H. Eberly, and N. P. Bigelow, Phys. Rev. A **59**, 1533 (1999).

[129] A. A. Svidzinsky and A. L. Fetter, Phys. Rev. A **62**, 063617 (2000).

[130] A. L. Fetter and J.-k. Kim, J. Low Temp. Phys. **125**, 239 (2001).

[131] D. V. Skryabin, Phys. Rev. A **63**, 013602 (2000).

[132] R. J. Dodd, K. Burnett, M. Edwards, and C. W. Clark, Phys. Rev. A **56**, 587 (1997).

[133] T. Isoshima and K. Machida, J. Phys. Soc. Jpn. **66**, 3502 (1997).

[134] W. Thomson, *Mathematical and Physical Papers* (Cambridge University Press, Cambridge, 1910), Vol. IV.

[135] M. Linn and A. L. Fetter, Phys. Rev. A **61**, 063603 (2000).

[136] A. A. Svidzinsky and A. L. Fetter, Phys. Rev. Lett. **84**, 5919 (2000).

[137] A. A. Svidzinsky and A. L. Fetter, Phys. Rev. A **58**, 3168 (1998).

[138] D. L. Feder, C. W. Clark, and B. I. Schneider, Phys. Rev. Lett. **82**, 4956 (1999).

[139] J. J. García-Ripoll and V. M. Pérez-García, Phys. Rev. A **60**, 4864 (1999).

[140] D. L. Feder, A. A. Svidzinsky, A. L. Fetter, and C. W. Clark, Phys. Rev. Lett. **86**, 564 (2001).

[141] J. J. García-Ripoll and V. M. Pérez-García, Phys. Rev. A **63**, 041603(R) (2001).

[142] A. Aftalion and T. Riviere, Phys. Rev. A **64**, 043611 (2001).

[143] M. Modugno, L. Pricoupenko, and Y. Castin, cond-mat/0203597v2, 2002.

[144] T. Isoshima and K. Machida, J. Phys. Soc. Jpn. **68**, 487 (1999).

[145] T. Isoshima and K. Machida, Phys. Rev. A **60**, 3313 (1999).

[146] J. R. Anglin, Phys. Rev. A **65**, 063611 (2002).

[147] B. Jackson, J. F. McCann, and C. S. Adams, Phys. Rev. A **61**, 013604 (1999).

[148] S. A. McGee and M. J. Holland, Phys. Rev. A **63**, 043608 (2001).

[149] G. B. Hess, Phys. Rev. **161**, 189 (1967).

[150] R. E. Packard and T. M. Sanders, Jr., Phys. Rev. A **6**, 799 (1972).

[151] B. Y. Rubinstein and L. M. Pismen, Physica D **78**, 1 (1994).

[152] H. Lamb, *Hydrodynamics* (Cambridge University Press, New York, 1975).

[153] D. J. Thouless, P. Ao, and Q. Niu, Phys. Rev. Lett. **76**, 3758 (1996).

[154] E. B. Sonin, Phys. Rev. B **55**, 485 (1997).

[155] T. Isoshima and K. Machida, Phys. Rev. A **59**, 2203 (1999).

[156] P. O. Fedichev and G. V. Shlyapnikov, Phys. Rev. A **60**, R1779 (1999).

[157] O. N. Zhuravlev, A. E. Muryshev, and P. O. Fedichev, Phys. Rev. A **64**, 053601 (2001).

[158] Y. Castin and R. Dum, Phys. Rev. Lett. **77**, 5315 (1996).

[159] E. Lundh, C. J. Pethick, and H. Smith, Phys. Rev. A **58**, 4816 (1998).

[160] F. Dalfovo and M. Modugno, Phys. Rev. A **61**, 023605 (2000).

[161] T. Nikuni, E. Zaremba, and A. Griffin, Phys. Rev. Lett. **83**, 10 (1999).

[162] L. I. Schiff, *Quantum Mechanics* (McGraw-Hill, New York, 1955).

[163] E. Šimánek, Phys. Rev. B **46**, 14054 (1992).

[164] M. Baert *et al.*, Europhys. Lett. **29**, 157 (1995).

[165] V. V. Moshchalkov *et al.*, Phys. Rev. B **54**, 7385 (1996).

[166] G. M. Braverman, S. A. Gredeskul, and Y. Avishai, Phys. Rev. B **57**, 13899 (1998).

[167] S. Hasegawa *et al.*, Phys. Rev. B **43**, 7631 (1991).

[168] P. L. Marston and W. M. Fairbank, Phys. Rev. Lett. **39**, 1208 (1977).

[169] T. Isoshima, private communication.

[170] I. Aranson and V. Steinberg, Phys. Rev. B **53**, 75 (1996).

[171] E. Lundh, Phys. Rev. A **65**, 043604 (2002).

[172] P. G. de Gennes, *Superconductivity of Metals and Alloys* (Addison-Wesley, Reading, Massachusetts, 1989).

[173] F. Gygi and M. Schlüter, Phys. Rev. B **43**, 7609 (1991).

[174] N. Hayashi, T. Isoshima, M. Ichioka, and K. Machida, Phys. Rev. Lett. **80**, 2921 (1998).

[175] F. V. De Blasio and Ø. Elgarøy, Phys. Rev. Lett. **82**, 1815 (1999).

[176] S. M. M. Virtanen and M. M. Salomaa, Physica B **284–288**, 741 (2000).

[177] T. P. Simula, S. M. M. Virtanen, and M. M. Salomaa, Comp. Phys. Comm. **142**, 396 (2001).

Abstracts of Publications I–VIII

I. We compute the structure of a quantized vortex line in a harmonically trapped dilute atomic Bose-Einstein condensate using the Popov version of the Hartree-Fock-Bogoliubov mean-field theory. The vortex is shown to be (meta)stable in a nonrotating trap even in the zero-temperature limit, thus confirming that weak particle interactions induce the condensed gas a fundamental property characterizing "classical" superfluids. We present the structure of the vortex at ultralow temperatures and discuss the crucial effect of the thermal gas component to its energetic stability.

II. We compute structures of vortex configurations in a harmonically trapped Bose-Einstein condensed atom gas within three different gapless self-consistent mean-field theories. Outside the vortex core region, the density profiles for the condensate and the thermal gas are found to differ only by a few percent between the Hartree-Fock-Bogoliubov-Popov theory and two of its recently proposed gapless extensions. In the core region, however, the differences in the density profiles are substantial. The structural differences are reflected in the energies of the quasiparticle states localized near the vortex core. Especially, the predictions for the energy of the lowest quasiparticle excitation differ considerably between the theoretical models investigated.

III. Considering a moving vortex line in a dilute atomic Bose-Einstein condensate within time-dependent Hartree-Fock-Bogoliubov-Popov theory, we derive a criterion for the quasiparticle excitations to follow the vortex core rigidly. The assumption of adiabaticity, which is crucial for the validity of the stationary self-consistent theories in describing such time-dependent phenomena, is shown to imply a stringent criterion for the velocity of the vortex line. Furthermore, this condition is shown to be violated in the recent vortex precession experiments.

IV. We study the stability of vortices in trapped single-component Bose-Einstein condensates within self-consistent mean-field theories—especially we consider the Hartree-Fock-Bogoliubov-Popov theory and its recently proposed gapless extensions. It is shown that for sufficiently repulsively interacting systems the anomalous negative-energy modes related to vortex instabilities are lifted to positive energies due to partial filling of the vortex core with noncondensed gas. Such a behavior implies that within these theories the vortex states are eventually stable against transfer of condensate matter to the anomalous core modes. This self-stabilization of vortices, shown to occur under very general circumstances, is contrasted to the predictions of the non-self-consistent Bogoliubov approximation, which is known to exhibit anomalous modes for all vortex configurations and thus implying instability of these states. In addition, the shortcomings of these approximations in

describing the properties of vortices are analysed, and the need of a self-consistent theory taking properly into account the coupled dynamics of the condensate and the noncondensate atoms is emphasized.

V. Multiply quantized vortices in trapped Bose-Einstein condensates are studied using the Bogoliubov theory. Suitable combinations of a localized pinning potential and external rotation of the system are found to energetically stabilize, both locally and globally, vortices with multiple circulation quanta. We present a phase diagram for stable multiply quantized vortices in terms of the angular rotation frequency and the width of the pinning potential. We argue that multiquantum vortices could be experimentally created using these two expedients.

VI. We present an efficient computational method to solve selfconsistently the Bogoliubov-de Gennes equations of weak coupling superconductivity. As a function of system size, the scaling of the CPU time required by the scheme is shown to be preferable compared to the methods commonly used. Also, the scheme allows taking into account nonlocal pairing interactions without additional computational cost. The favourable scaling behavior enables computation of microscopic electronic structures for ranges of physical parameter values previously inaccessible.

VII. Superconducting quasiparticle excitation spectra are computed for m times quantized flux lines using a self-consistent Bogoliubov-de Gennes approach. We find m discrete branches of bound-state solutions in the spectrum, corresponding to different values of the quasiparticle angular momentum. Owing to the bound states, the STM tunneling conductance of the vortex is predicted to display m rows of peaks as a function of the distance from the vortex axis.

VIII. The electronic structure of domain walls in superconductors is computed as a function of temperature within Bogoliubov-de Gennes theory. We find a spontaneous interface transition at an ultralow temperature $T_\star \approx 10^{-2}T_\mathrm{c}$, in which the selfconsistent pair potential transforms from smooth Ginzburg-Landau form into oscillatory Friedel-like behavior. The transition is associated with a lifting of the energy of midgap excitations and the formation of an energy minigap. Alike the bulk superconducting phase transition at T_c, this midgap transition is manifested with a pronounced peak in the specific heat of domain-wall matter. The transition is also predicted to occur in thin SNS Josephson junctions.

ISBN 951-22-6427-7
ISSN 1456-3320